

This is the peer-reviewed, manuscript version of an article published in the *Journal of Proteomics*. The version of record is available from the journal site:

<https://doi.org/10.1016/j.jprot.2017.11.007>.

© 2017. This manuscript version is made available under the CC-BY-NC-ND 4.0 license

<http://creativecommons.org/licenses/by-nc-nd/4.0/>.

The full details of the published version of the article are as follows:

TITLE: Integrative transcriptome and proteome analyses define marked differences between *Neospora caninum* isolates throughout the tachyzoite lytic cycle

AUTHORS: Horcajo, P., **Xia, D.**, Randle, N., Collantes-Fernández, E., Wastling, J., Ortega-Mora, L. M. and Regidor-Cerrillo, J.

JOURNAL: Journal of Proteomics

PUBLISHER: Elsevier

PUBLICATION DATE: 14 November 2017 (online)

DOI: 10.1016/j.jprot.2017.11.007

1 **Integrative transcriptome and proteome analyses define marked differences**
2 **between *Neospora caninum* isolates throughout the tachyzoite lytic cycle**

3

4 P. Horcajo^{1‡}, D. Xia^{2‡}, N. Randle³, E. Collantes-Fernández¹, J. Wastling⁴, L.M. Ortega-
5 Mora¹, J. Regidor-Cerrillo^{1*}.

6 ¹ SALUVET, Animal Health Department, Faculty of Veterinary Sciences, Complutense
7 University of Madrid, Ciudad Universitaria s/n, 28040 Madrid, Spain.

8 ² The Royal Veterinary College, Royal College Street, London, NW1 0TU, United
9 Kingdom.

10 ³ Department of Infection Biology, Institute of Infection & Global Health, University of
11 Liverpool, Liverpool Science Park IC2, 146 Brownlow Hill, Liverpool, L3 5RF, United
12 Kingdom.

13 ⁴ Faculty of Natural Sciences, Keele University, Keele, Staffordshire, ST5 5BG, United
14 Kingdom.

15 [‡]Authors contributed equally

16 *Corresponding author: Javier Regidor Cerrillo, Animal Health Department, Faculty of
17 Veterinary Sciences, Complutense University of Madrid, Ciudad Universitaria s/n 28040,
18 Madrid, Spain. E-mail: jregidor@ucm.es

19

20

21 Co-authors e-mail addresses: PH: phorcajo@ucm.es; DX: dxia@rvc.ac.uk; NR:
22 Nadine.Randle@liverpool.ac.uk; ECF: esthercf@ucm.es; JW: j.wastling@keele.ac.uk;
23 LMOM: luis.ortega@ucm.es; JRC: jregidor@ucm.es

24

25 **Abstract**

26 *Neospora caninum* is one of the main causes of transmissible abortion in cattle. Intraspecific
27 variations in virulence have been widely shown among *N. caninum* isolates. However, the
28 molecular basis governing such variability have not been elucidated to date. In this study label
29 free LC-MS/MS was used to investigate proteome differences between the high virulence isolate
30 Nc-Spain7 and the low virulence isolate Nc-Spain1H throughout the tachyzoite lytic cycle. The
31 results showed greater differences in the abundance of proteins at invasion and egress with 77 and
32 62 proteins, respectively. During parasite replication, only 19 proteins were differentially
33 abundant between isolates. The microneme protein repertoire involved in parasite invasion and
34 egress was more abundant in the Nc-Spain1H isolate, which displays a lower invasion rate.
35 Rhoptry and dense granule proteins, proteins related to metabolism and stress responses also
36 showed differential abundances between isolates. Comparative RNA-seq analyses during
37 tachyzoite egress were also performed, revealing an expression profile of genes associated with
38 the bradyzoite stage in the low virulence Nc-Spain1H isolate. The differences in proteome and
39 RNA expression profiles between these two isolates reveal interesting insights into likely
40 mechanisms involved in specific phenotypic traits and virulence in *N. caninum*.

41

42 **Keywords:** *Neospora caninum*, Low and high virulence isolates, Proteome,
43 Transcriptome

44

45 **1. Introduction**

46 *Neospora caninum* is a cyst-forming obligate intracellular protozoan parasite that is
47 closely related to *Toxoplasma gondii*, which infects different domestic or wild canids as
48 its definitive host and cattle and other ungulates as intermediate hosts [1]. *N. caninum* has
49 been recognized as one of the main causes of abortion in cattle, resulting in devastating
50 economic losses to the beef and dairy industries [2]. Although various factors are
51 potentially involved in determining the dynamics of *N. caninum* infection, experiments
52 in pregnant cattle have shown the key role of different isolates of *N. caninum* in the
53 severity of disease and its capacity to cause foetal mortality in cattle [3-6]. Host tissue
54 damage occurs as a consequence of the tachyzoite lytic cycle, a process that enables
55 parasite propagation and involves the following successive steps: parasite invasion,
56 adaptation to new intra-cytoplasmatic conditions, intracellular proliferation and egress
57 from host cells [7,8]. Interestingly, the *in vitro* behaviour of a *N. caninum* population in
58 these processes has demonstrated the potential association of the phenotypic traits such
59 as the invasion rate and tachyzoite yield with pathogenicity observed in animal models
60 [9-11]. Nevertheless, the molecular basis and mechanisms that govern such biological
61 diversity in *N. caninum* remain largely unknown. *N. caninum* appears to be highly
62 conserved genetically [12], although previous proteomic approaches have identified some
63 differences between isolates [13-15]. Differences in secretory elements (rhoptry and
64 dense granule proteins) and protein related to gliding motility and oxidative stress have
65 been described among *N. caninum* isolates showing variations in protein expression, post-
66 translational modifications and protein turnover [15]. Recently, an *in vitro* study
67 comparing host cell modulation by *N. caninum* isolates with high (Nc-Spain7) and low
68 (Nc-Spain1H) virulence has shown a great similarity in host transcriptome modulation by
69 both isolates but marked differences in the parasite transcriptome between isolates [16].

70 In this study, we used a global approach to examine the changes between the *N. caninum*
71 Nc-Spain7 and Nc-Spain1H isolates throughout the fast replicating tachyzoite lytic cycle.
72 We exploited label free LC-MS/MS technology to investigate in deep proteome
73 differences across the tachyzoite lytic cycle: after tachyzoite invasion and adaptation in
74 the host cell at 12 hours post infection (hpi), during active parasite replication at 36 hpi
75 and at early egress at 56 hpi. Furthermore, we analysed the transcriptome status of Nc-
76 Spain7 and Nc-Spain1H using RNA-seq during tachyzoite egress from the host cell. We
77 determined specific patterns of protein abundance for each isolate in each phase of the
78 lytic cycle studied and differences between gene expression profiles that reveal
79 interesting insights into differences in virulence between these two isolates.

80

81 **2. Materials and methods**

82 2.1 Parasite culture

83 Parasites were cultured in confluent Marc-145 cultures as previously described [17].
84 Briefly, medium from Marc-145 cultures grown for 24 h in DMEM with 10% of heat
85 inactivated FBS and 1% antibiotic-antimycotic solution (Gibco, Gaithersburg, MD, USA)
86 was replaced with DMEM supplemented with 2% FCS and 1% of antibiotic-antimycotic
87 solution. Then, cell monolayers were inoculated with an adjusted multiplicity of infection
88 (MOI) of Nc-Spain1H and Nc-Spain7 tachyzoites for parasite passaging onto a new
89 Marc-145 monolayer each three – four days. All experiments in this study were conducted
90 with tachyzoites from both isolates with a limited number of passages (Nc-Spain1H and
91 Nc-Spain7, passage 13-18). All inoculations in *in vitro* assays were performed within one
92 hour after tachyzoite collection from flasks.

93 2.2 Experimental design and tachyzoite production for proteome and transcriptome 94 analyses

95 The overall experimental design is shown in Fig. 1. All experiments were carried out with
96 three biological replicates.

97 Confluent 24-h Marc-145 DMEM free of phenol red (Gibco, Gaithersburg, MD, USA)
98 and FBS were inoculated with purified Nc-Spain1H tachyzoites at a MOI of 7 and Nc-
99 Spain7 tachyzoites at a MOI of 4. Cell monolayers were recovered at 12 hpi (after
100 completion of invasion and prior to tachyzoite duplication), at 36 hpi (active proliferation
101 in the parasitophorous vacuole) and at 56 hpi (early egress), from T75 cm² flasks by cell
102 scraping in 5 ml of PBS supplemented with protease and phosphatase inhibitor cocktail
103 (Sigma-Aldrich, St. Louis, MO, USA), passaged by 25 G needles for host cell disruption
104 and purified using PD-10 (Sephadex G-25 columns -GE-Healthcare, Barrington, IL,
105 USA). Tachyzoite purification was carried out at 4°C. The number and viability of
106 tachyzoites was determined by trypan blue exclusion followed by counting in a Neubauer
107 chamber. Tachyzoites were pelleted by centrifugation at 1,350 x g for 10 min. and stored
108 at – 80°C until tachyzoite proteome (TZP) analysis.

109 Tachyzoite samples for transcriptome analysis were obtained as described above. Cell
110 cultures were recovered at 56 hpi, and tachyzoites were purified using PD10 columns as
111 described above. Tachyzoite pellets were directly resuspended in 300 µl of RNAlater
112 (Invitrogen, Carlsbad, CA, USA) and stored at – 80°C until RNA extraction.

113 The tachyzoite growth and lytic cycle was monitored daily by microscopy, and
114 photomicrographs for each time-point of sample collection were obtained at 400x on an
115 inverted microscope (Nikon Eclipse E400) connected to a digital camera for checking
116 lytic cycle progression and sample collection in the programmed lytic cycle phases
117 (Fig.1A).

118 2.3 LC-MS/MS analyses

119 Detailed materials and methods for sample preparation, LC-MS/MS, proteome data
120 analysis, and Western blot validation are shown in Supplementary file 1. Briefly, prior to
121 trypsin digestion, tachyzoite pellets were resuspended in 25 mM ammonium bicarbonate
122 and RapiGestTM (Waters MS Technologies, Milford, MA, USA) for protein
123 solubilization, reduced with DTT and alkylated with iodoacetamide for trypsin digestion.
124 Then, the digests were analysed using an LC-MS/MS system comprising an Ultimate
125 3000 nano system coupled to a Q-Exactive mass spectrometer (Thermo Fisher Scientific,
126 Waltham, MA, USA). Reversed-phase liquid chromatography was performed using the
127 Ultimate 3000 nanosystem by a linear gradient of 5-40% solvent B (80% acetonitrile in
128 0.1% formic acid) in 0.1% formic acid (solvent A). The Q-Exactive was operated in data-
129 dependent mode with survey scans acquired at a resolution of 70,000 at m/z 200. Up to
130 the top 10 most abundant isotope patterns were selected and fragmented by higher energy
131 collisional dissociation with normalized collision energies of 30. The maximum ion
132 injection times for the survey scan and the MS/MS scans were 250 and 100 ms,
133 respectively.

134 For proteome data analyses, the Thermo RAW files were imported into Progenesis QI
135 (version 2.0, Nonlinear Dynamics, Durham, CA, USA). Replicate runs were time-aligned
136 using default settings and an auto-selected run as a reference. Spectral data were
137 transformed into .mgf files with Progenesis QI and exported for peptide identification
138 using the Mascot (version 2.3, Matrix Science, London, UK) search engine and the
139 database ToxoDB-26_*Ncaninum* LIV_Annotated Proteins (version 26, ToxoDB). The
140 false discovery rates were set at 1% and at least two unique peptides were required for
141 reporting protein identifications. Finally, protein abundance (iBAQ) was calculated as the
142 sum of all the peak intensities (from the Progenesis output) divided by the number of
143 theoretically observable tryptic peptides for a given protein (Fig. 1B).

144 The mass spectrometry proteomics data have been deposited in the ProteomeXchange
145 Consortium via the PRIDE [18] partner repository with the dataset identifier PXD007062.
146 The identified proteins were classified according to their parasite localization and
147 functionality according to the Gene Ontology (GO) terms (annotated and predicted) on
148 the ToxoDB website [19] for the Nc-Liverpool isolate (ToxoDB-
149 26_NcaninumLIV_AnnotatedProteins), *T. gondii* syntenic homologues (version 26,
150 ToxoDB) and previous reports [20-22].

151 Validation of LC-MS/MS results was performed by measuring the differential abundance
152 of the proteins MIC2 (NCLIV_022970), ROP2 (NCLIV_001970), and NTPase
153 (NCLIV_068400) between isolates by Western blot analyses using the SAG1 protein
154 (NCLIV_033230) as a housekeeping gene as previously described [23,24]. Images from
155 WB membranes were obtained using a GS-800 Scanner (Bio-Rad Laboratories, Hercules,
156 CA, USA) and were analysed with Quantity One quantification software v. 4.0 (Bio-Rad
157 Laboratories, Hercules, CA, USA) for protein quantification.

158 2.4 RNA extraction, sequencing and detection of differential mRNA expression

159 Total RNA was isolated from purified tachyzoites using an RNeasy Mini kit (Qiagen,
160 Hilden, Germany). RNA-Seq was undertaken at the Centre for Genomic Research,
161 University of Liverpool. Briefly, polyadenylated RNA was purified using the
162 Dynabeads® mRNA purification kit (Invitrogen, Carlsbad, CA, USA) and used to
163 prepare RNA-Seq libraries with the Epicentre ScriptSeq v2 RNA-Seq Library Preparation
164 kit (Illumina, San Diego, CA, USA). Libraries were sequenced on the HiSeq2500
165 (Illumina, San Diego, CA, USA) as 2 x 100-bp paired-end sequencing using rapid-run
166 mode chemistry. Filtered sequencing reads were aligned against the reference genome of
167 *N. caninum* (NcLiv26; ToxoDB.org) by the TopHat2 aligner and processed with the

168 Cufflinks software (version 2.1.1) to assemble transcripts, quantify expression levels and
169 analyse differentially expressed genes (DEGs) (Fig. 1C).

170 Validation of transcript expression was performed on three additional biological
171 replicates of tachyzoite samples at 56 hpi prepared as described above using SYBR green
172 quantitative PCR. More detailed material and methods for RNAseq and validation by
173 quantitative real-time PCR are provided in Supplementary file 1.

174 2.5 *In vitro* invasion analysis

175 The invasion capacity of *N. caninum* isolates was determined in a plaque assay in which
176 100 purified tachyzoites of each isolate per well were added to MARC-145 monolayers
177 in 24-well culture plates as previously described [10]. Briefly, the plates were incubated
178 at 37°C in a 5% CO₂-humidified incubator for 48 h, and cell monolayers were labelled
179 by immunofluorescence using anti-tachyzoite hyperimmune rabbit antiserum (1:4000) as
180 the primary antibody and Alexa 594-conjugated goat anti-rabbit secondary antibody
181 (1:1000) (Molecular Probes, Eugene, Oregon, USA). Plate wells were examined using a
182 fluorescence-inverted microscope Nikon Eclipse E400 (Nikon Instruments Europe) at a
183 magnification of 200x to count the labelled parasitophorous vacuoles and lysis plaques
184 (events) per well after parasite growth. Differences between isolates in invasion rates
185 were determined using the U Mann-Whitney test.

186 2.6 Tachyzoite cell cycle analysis

187 The cell cycle phase of the tachyzoite culture was studied by flow cytometry. Tachyzoite
188 samples were obtained under the same conditions as detailed previously for proteomic
189 and transcriptome analyses. Purified tachyzoites were pelleted for 10 min at 1350×g and
190 resuspended in 70% (v/v) ethanol with constant shaking, pelleted and resuspended in
191 PBS. Fixed tachyzoites were labelled by indirect immunofluorescence (IFI) for the
192 differentiation of individual parasites from those forming aggregates. Tachyzoites were

193 permeabilised with PBS containing 3% BSA and 0.25% Triton X-100 for 30 min at 37°C
194 and labelled using anti-tachyzoite mouse antiserum (1:50 dilution) as the primary
195 antibody and a FITC-conjugated goat anti-mouse IgG at 1:1,000 dilution (Molecular
196 Probes, Eugene, Oregon, USA) as the secondary antibody. Then, the parasites were
197 treated with 250 U RNase A (Ambion, Austin, TX, USA) in the dark for 30 min,
198 resuspended in BD CellFIX™ (Becton-Dickinson, Erembodegem, Belgium), and stained
199 with propidium iodide (PI) (1 µg/ml final concentration). Tachyzoite populations with
200 lower FITC fluorescence were separated as individual tachyzoites. The nuclear DNA
201 content was measured based on the PI fluorescence using a 488 nm argon laser and a
202 Becton-Dickinson FACSCalibur flow cytometer (Becton-Dickinson, Erembodegem,
203 Belgium). Fluorescence was collected in linear mode (10 000 events), and the results were
204 quantified using CELLQuest™ v3.0 (Becton-Dickinson, Erembodegem, Belgium). The
205 percentages of G1 (1 N), S (1–2 N) and G2+M (2 N) tachyzoites were calculated based
206 on defined gates for each population. Two biological replicates were analysed for each
207 isolate.

208

209 **3. Results and discussion**

210 3.1 Nc-Spain1H and Nc-Spain7 tachyzoite proteomes resemble fast-growing,
211 metabolically active and invasive tachyzoites

212 A total of 1,390 proteins were identified with high confidence (FDR < 1% and containing
213 at least two uniquely identified peptides) and quantified using Progenesis software for the
214 Nc-Spain1H and Nc-Spain7 isolates across the tachyzoite lytic cycle. The identified
215 proteins covered ~19.6% of the predicted *N. caninum* proteins deposited in the UniProt
216 database (7,111 predicted proteins, UniProtKB; UP000007494, *Neospora caninum* strain
217 Liverpool) [25]. Raw data are deposited in ProteomeXchange under identifier

218 PXD007062. Each individual identified and quantified protein was categorized by the
219 cellular component and functional prediction. Of the proteins, 14.5% had an unknown
220 localization. Proteins with cytoplasmic (18.49%), nuclear (16.26%) and mitochondrial
221 (11.15%) localizations were also highly represented, followed by proteins associated with
222 the plasma membrane (glycolipid-anchored SAG1-related sequences [SRS] and other
223 proteins localized in the plasma membrane) (9.78%). Proteins from secretory organelles
224 (including micronemes, rhoptries and dense granules) represented approximately 5%
225 (corresponding to 70 proteins) of all those identified proteins (Supplementary Fig. 1A and
226 supplementary file 2). A total of 66.47% of 1,390 proteins from the TZP were assigned
227 to a functional category (Supplementary Fig. 1B and supplementary file 2). The most
228 represented functional categories included proteins involved in metabolism (12%),
229 cellular transport (10%), protein synthesis (9.57%) and protein fate (9.35%). As expected,
230 protein localization and functional profiles identified in both *N. caninum* isolates
231 corresponded to the proteome for the fast growing, metabolically active and invasive
232 tachyzoites.

233 3.2 Relative quantification demonstrated different proteomes for Nc-Spain1H and Nc- 234 Spain7 throughout the tachyzoite lytic cycle

235 Progenesis analysis detected 351 proteins at 12 hpi, 136 proteins at 36 hpi and 214
236 proteins at 56 hpi, with a significant increase or decrease in relative abundance between
237 Nc-Spain1H and Nc-Spain7 TZPs ($q < 0.05$) (Supplementary file 3). These results
238 demonstrated marked differences in the TZP throughout the lytic cycle between the Nc-
239 Spain1H and Nc-Spain7 isolates. Focusing on significant changes ($q < 0.05$) in the
240 relative abundance with a fold change ≥ 2 between the Nc-Spain1H and Nc-Spain7
241 isolates, there were 77, 19 and 62 proteins with differing abundance at 12, 36 and 56 hpi,
242 respectively (Fig. 2A, B and C, respectively and Supplementary file 3). Most of the

243 proteins that were differentially abundant between isolates were unique to each time-point
244 of the tachyzoite lytic cycle (Fig. 3 and supplementary file 4). There were only 7 out of
245 82 Nc-Spain1H proteins and 2 out of 36 Nc-Spain7 proteins that were consistently more
246 abundant across the tachyzoite lytic cycle.

247 Enriched GO terms or pathways associated with a particular isolate were not found likely
248 due to the high proportion of hypothetical proteins. Nonetheless, differences in the
249 abundance of proteins belonging well-established categories related with invasion
250 machinery, metabolism and response to stress were found between isolates and are
251 detailed below (Fig. 4).

252 The proteome results from LC-MS/MS were confirmed by WB analyses with available
253 antibodies. The WB results provided similar results to the LC-MS/MS quantification with
254 a higher abundance of NcMIC2 at 12 and 56 hpi in the Nc-Spain1H isolate and a similar
255 protein abundance of NcROP2 and NcNTPase in both isolates (Supplementary Fig. 2).

256 3.3 Abundance of proteins involved in host cell attachment and invasion varied between
257 Nc-Spain1H and Nc-Spain7 tachyzoite proteomes

258 *Surface antigens differ in abundance between Nc-Spain1H and Nc-Spain7 tachyzoite*
259 *proteomes.*

260 Members of the SRS protein family were differentially abundant between the Nc-
261 Spain1H and Nc-Spain7 isolates. SRS antigens exert a relevant role in host cell
262 attachment, modulation and evasion of host immunity, and the regulation of virulence
263 [26-28]. An orthologue of, but not syntenic to, TgSAG3 (NCLIV_034740) throughout the
264 tachyzoite lytic cycle and an orthologue of SRS67 (NCLIV_046140) at 56 hpi were
265 significantly more abundant in Nc-Spain1H. More interestingly, NcSAG4
266 (NCLIV_019580) showed larger fold changes at all time-points in Nc-Spain1H, with the
267 greatest differences compared with Nc-Spain7 at 36 and 56 hpi (12.8-fold and 14.6-fold,
268 respectively). NcSAG4 has been described as a *N. caninum* bradyzoite stage-specific

269 marker [29]. Furthermore, SRS6 (NCLIV_010050), which has been found over-
270 expressed in bradyzoites of *T. gondii* [30], was also significantly more abundant in Nc-
271 Spain1H at 56 hpi. Bradyzoite development of *T. gondii* has been correlated with a
272 reduction in the tachyzoite growth rate [31]. Nc-Spain1H has shown a low *in vitro* growth
273 rate [9] which may facilitate the conversion to the bradyzoite, although has been
274 previously shown that Nc-Spain1H produce only intermediate bradyzoites *in vitro* [32].
275 The transcriptome analysis, which is detailed in the next section, could corroborate the
276 hypothesis of a pre-bradyzoite stage in Nc-Spain1H since an important bradyzoite gene
277 profile was found to be over-expressed in this isolate. The only SRS protein that was more
278 abundant in Nc-Spain7 throughout the lytic cycle was the orthologue of SRS39
279 (NCLIV_023620), which is also predominantly expressed during the bradyzoite stage of
280 in the *T. gondii* [30]. It could be interesting to determine the relevance of SRS39 in *N.*
281 *caninum*.

282 *The microneme protein repertoire is more abundant in Nc-Spain1H tachyzoites, but Nc-*
283 *Spain1H displays a lower invasion rate.*

284 Micronemes in Apicomplexan parasites are specialized secretory organelles that are
285 critical for essential cellular processes such as attachment and penetration [33]. A total of
286 9 microneme (MIC) proteins were significantly more abundant in Nc-Spain1H at 56 hpi,
287 and most of them were also more abundant in Nc-Spain1H at 12 hpi, four with FC > 2
288 and the other four with FC very close to 2 (> 1.8). Only MIC8 (NCLIV_062770) had a
289 higher abundance at 12 hpi but not at 56 hpi. At 36 hpi, differences in the abundance of
290 MIC proteins were not found. Among MIC proteins with higher abundance in Nc-
291 Sapin1H, orthologues assembling the main TgMIC complexes (MIC1
292 [NCLIV_043270]/MIC4 [NCLIV_002940] /MIC6; MIC2 [NCLIV_022970]/M2AP
293 [NCLIV_051970]; and MIC8 [NCLIV_062770]/MIC3 [NCLIV_010600]) and others as

294 MIC2-like1 (NCLIV_033690), MIC10 (NCLIV_066250), MIC11 (NCLIV_020720) and
295 MIC17B (NCLIV_038110) were identified. Some of these proteins have been
296 characterized in *N. caninum* and have been associated with invasion processes [34-37].
297 In contrast to these results, in previous work comparing changes in the proteome
298 expression between these two isolates using DIGE, NcMIC1 was found more abundant
299 in the highly virulent isolate Nc-Spain7 [15]. However, these contrasting results are likely
300 due to differences in techniques, considering that DIGE analysis detects variations in
301 protein species that are likely also attributed to post-translational modifications.
302 NcAMA1 (NCLIV_028680), which is also involved in *N. caninum* invasion [38], was
303 also increased in Nc-Spain1H TZP at 12 and 56 hpi.

304 In addition to MIC proteins, proteases involved in micronemal protein processing or that
305 contribute to microneme-dependent processes, such as egress, gliding motility, and
306 parasite invasion of host cells, were also more abundant in Nc-Spain1H. Orthologues of
307 the protease SUB1 (NCLIV_021050), which is involved in micronemal protein
308 processing [39], the metalloproteinase toxolysin 4, TLN4, (NCLIV_044230) and the
309 cathepsin L-like protease CPL (NCLIV_004380), proteinase localized outside the
310 micronemes in the vacuolar component, which in *T. gondii* contributes to the proteolytic
311 maturation of proTgM2AP and proTgMIC3 [40], were also found more abundant in Nc-
312 Spain1H at 12 hpi (SUB1) and at 56 hpi (SUB1, TLN4 and CPL). Similarly, PLP1
313 (NCLIV_020990), a perforin-like protein secreted from micronemes that likely plays a
314 role in parasite egress more than invasion [41], and an orthologue of the chitinase-like
315 protein CLP1 (NCLIV_000740) related to macrophage stimulation to release pro-
316 inflammatory cytokines in *T. gondii* [42], were more abundant in Nc-Spain1H at 12
317 (PLP1) and at 56 hpi (PLP1 and CLP1).

318 All these results seem to indicate that the low virulent isolate Nc-Spain1H has powerful
319 machinery involved in host cell attachment and invasion. In this study, we tested the
320 ability of Nc-Spain1H and Nc-Spain7 to invade host cells. The Nc-Spain1H showed a
321 significant reduction of host invasion ($p < 0.005$) in comparison to Nc-Spain7 (Fig. 5A),
322 as demonstrated in previous work [9,11]. Considering these results, the Nc-Spain1H
323 isolate may be compromised in other unknown mechanisms that are relevant for
324 attachment/invasion processes and the over-expression of all of these factors could be an
325 attempt to compensate for some other deficiency.

326 *Rhoptry proteins also differ in abundance between isolates.*

327 Rhoptry proteins are recognized as one of the major virulence factors in *T. gondii* [43,44].
328 Three proteins from rhoptries had different abundances between isolates. NcROP1
329 (NCLIV_069110), which is involved in early invasion [45], showed an approximately 2-
330 fold higher abundance in Nc-Spain1H at 12 and 56 hpi. Interestingly, a predicted member
331 of the rhoptry kinase family ROP20 specific for *N. caninum* (NCLIV_068850), which is
332 orthologous, but not syntenic, to the *T. gondii* virulence factor ROP24 had greater
333 abundance in the highly virulent isolate Nc-Spain7 across the lytic cycle. The orthologue
334 of the bradyzoite pseudokinase 1, BPK1 (NCLIV_007770) was also more abundant in the
335 Nc-Spain7 isolate across the lytic cycle. BPK1 plays a crucial role in the *in vivo*
336 development of *Toxoplasma* cysts [46]. The abundances of BPK1 and SRS39 in Nc-
337 Spain7 are inconsistent with those other bradyzoite-related proteins that were more
338 abundant in the Nc-Spain1H. It remains to be determined if there is a functional role for
339 these proteins in the tachyzoite stage of *N. caninum*.

340 3.4 Metabolic processes are differentially regulated between Nc-Spain1H and Nc-Spain7
341 isolates

342 *Gluconeogenesis is up-regulated in the low virulent isolate Nc-Spain1H*

343 Eleven proteins related to carbohydrate metabolism were differentially abundant between
344 isolates, with the greatest differences at 12 hpi. Ten proteins were more abundant in Nc-
345 Spain1H: fructose-1,6-bisphosphatase (NCLIV_050070), fructose-1,6-bisphosphatase
346 class 1 (NCLIV_050080), glycerol-3-phosphate dehydrogenase (NCLIV_001180),
347 phosphoglucomutase (NCLIV_010960), phosphoenolpyruvate carboxykinase
348 (NCLIV_041900), glucosamine:fructose-6-phosphate aminotransferase
349 (NCLIV_031610), cytochrome c (NCLIV_060860) and orthologues of aspartate
350 aminotransferase (NCLIV_064760), glycosyltransferase (NCLIV_004200) and citrate
351 synthase I (NCLIV_037460), which showed a 2-2.7-fold higher abundance in Nc-
352 Spain1H. During exponential growth (36 hpi), only the glucosamine-fructose-6-
353 phosphate aminotransferase (NCLIV_031610) was 2-fold more abundant in Nc-Spain1H.
354 At 56 hpi, there were no differences in these proteins between the isolates. Some of these
355 proteins suggest that Nc-Spain1H fulfils a gluconeogenic function. Co-expression of
356 enzymes involved in glycolysis and gluconeogenesis is a mechanism to rapidly adapt to
357 changing nutrient conditions in their host cells [47] and could be an important glucose
358 regulatory mechanism [48]. Over-expression of the function of gluconeogenesis in Nc-
359 Spain1H may also indicate a failure in glucose salvage from the host cell and thus could
360 be an important limiting factor for parasite growth. In relation to this hypothesis, the
361 orthologue of the transporter/permease protein related to carbohydrate transport
362 (NCLIV_039290) was more abundant in the highly virulent isolate Nc-Spain7 (3.3-fold).
363 This carbohydrate transporter in Nc-Spain7 could facilitate the capture of glucose from
364 the host and consequently the faster growth of this isolate.

365 *Fatty acid biosynthesis in the apicoplast (FAS II system) and the metabolism of*
366 *phospholipids are differentially regulated between isolates.*

367 The apicoplast is indispensable for parasite survival and is the location of several anabolic
368 pathways such as type II fatty acid [49]. Interestingly, orthologues of apicoplast triose

369 phosphate translocator APT1 (NCLIV_026210) and beta-hydroxyacyl-acyl carrier
370 protein dehydratase FABZ (NCLIV_004340), showed 2.8 and 2.4-fold higher abundance,
371 respectively, in Nc-Spain7 at 12 hpi. The APT1 was again more abundant in Nc-Spain7
372 (2.3-fold) at 56 hpi. In *T. gondii*, APT1 is required for fatty acid synthesis in the
373 apicoplast, but it also supplies the apicoplast with carbon skeletons for additional
374 pathways and indirectly with ATP and redox equivalents [50]. In addition, APT1 has been
375 shown to be an essential protein for parasite survival in *Toxoplasma* and *Plasmodium*.
376 Conversely, it is striking that the low virulence isolate Nc-Spain1H exhibited up-
377 regulated recycling of the phospholipids pathway, (LAMP, <http://www.llamp.net>) at 36
378 and 56 hpi. Lipin protein (NCLIV_031190) and the glycerol-3-phosphate acyltransferase
379 (NCLIV_029980) had 2.3 and 2.2-fold higher abundances, respectively, in Nc-Spain1H
380 at 36 hpi. At 56 hpi, the glycerol-3-phosphate acyltransferase (NCLIV_029980) and the
381 acyl-CoA synthetase (NCLIV_054250) had a 2-fold increased abundance in Nc-Spain1H.
382 Phospholipids are the major lipid components of biological membranes, but lipids also
383 serve as signalling molecules, energy stores, post-translational modifiers, and
384 pathogenesis factors. It might be interesting to assess whether this up-regulation of
385 proteins in Nc-Spain1H may be a strategy to counteract the effect of the lack of an
386 apicoplast contribution.
387 All these metabolic differences between isolates could, at least partially, explain their
388 phenotypic variations in growth if, as in *T. gondii*, strain-specific growth rates and
389 virulence are driven by altered metabolic capacities [51].

390 3.5 Other key biological systems are also differentially represented between isolates.

391 *Antioxidant and stress response systems*

392 In *N. caninum* the importance of the production of IFN-gamma-induced NO in
393 macrophages as a mechanism for killing intracellular *N. caninum* has been demonstrated

394 [52]. To counteract this oxidative stress, parasites are equipped with specific ROS-
395 detoxifying mechanisms that are critical for parasite survival and the establishment of
396 infection [53]. The superoxide dismutase SOD2 (NCLIV_058830) had a 2-fold higher
397 abundance in Nc-Spain1H TZP at 12 hpi. SOD2 in *T. gondii* is dually targeted to both the
398 apicoplast and the mitochondrion of *T. gondii*, two organelles that require protection from
399 oxidative stress [54]. Other proteins with oxidoreductase activity, such as the pyridine
400 nucleotide-disulphide oxidoreductase family protein (NCLIV_029160), also showed a
401 higher abundance in Nc-Spain1H at 12 hpi.

402 By contrast, another well-known antioxidant enzyme, the peroxiredoxin-2E-1
403 (NCLIV_014020), was more abundant in Nc-Spain7 throughout the entire tachyzoite
404 lytic cycle. Peroxiredoxins provide another defence mechanism against oxidative damage
405 and, in addition, some peroxiredoxins have been proposed as important
406 immunomodulators in parasites [55,56]. Additionally, the putative serine/threonine
407 protein phosphatase 5 (NCLIV_066900) and the orthologue of the NAD/NADP
408 octopine/nopaline dehydrogenase (NCLIV_042450) displayed higher abundance in Nc-
409 Spain7 at 12 hpi (2-2.5-fold) and 56 hpi (2.7-fold), respectively.

410 These findings could suggest that different ROS-detoxifying mechanisms are used by the
411 different *N. caninum* isolates, which may contribute to their differing resistances to the
412 host immune response.

413 Heat shock proteins are other stress-inducible proteins that can have important roles in
414 parasite survival, although their functions are still unknown. Stress conditions associated
415 with bradyzoite development induce the expression of HSPs such as HSP70 and HSP90
416 and HSP21 in *T. gondii* [57-59]. In the present work, the orthologue of HSP29
417 (NCLIV_041850), which is associated with the membrane of *T. gondii* [60], was 2-fold
418 more abundant in Nc-Spain1H at 12 hpi.

419 *Ubiquitin-proteasome system.*

420 The ubiquitin-proteasome system plays a role the biological processes of parasites such
421 as differentiation, cell cycle progression, proliferation and encystation [61]. The
422 orthologue of serine carboxypeptidase s28 protein (NCLIV_008320) and peptidase,
423 S9A/B/C family (NCLIV_063570), proteins related to the proteasome demonstrated a
424 higher abundance at 36 (2.6 and 2.4-fold, respectively) and 56 (3.6 and 2.5-fold,
425 respectively) hpi in Nc-Spain1H than in Nc-Spain7. Conversely, the ubiquitin family
426 domain-containing protein (NCLIV_012950) and ubiquitin conjugation factor
427 (NCLIV_019660), which are related to the ubiquitination process, were 2-fold more
428 abundant in Nc-Spain7 at 56 hpi. In *T. gondii*, proteasome inhibitors do not affect host
429 cell invasion but block parasite proliferation, daughter-cell budding, as well as DNA
430 synthesis [61]. Furthermore, a study of the ubiquitin proteome of *T. gondii* has revealed
431 a large number of ubiquitinated proteins localized to the cytoskeleton and inner
432 membrane complex, as well as their roles as critical regulators of cell division and cell
433 cycle transitions [62].

434 3.6 Nc-Spain1H and Nc-Spain7 tachyzoite transcriptome also showed marked variations
435 between isolates but were inconsistent with the proteome results

436 We also investigated the transcriptome of Nc-Spain1H and Nc-Spain7 during early egress
437 (56 hpi). Differential expression analysis revealed 550 DEGs between Nc-Spain1H and
438 Nc-Spain7. Among these genes, 369 were over-expressed in Nc-Spain1H and 181 in Nc-
439 Spain-7 (Supplemental file 5). The qPCR for RNA-Seq validation displayed a profile
440 similar to the RNA-Seq results, with a similar significance and direction of fold change
441 in the nine genes analysed (Supplementary Fig. 3).

442 Furthermore, a comparison of the differentially expressed transcripts and the
443 differentially expressed proteins at the same time-point showed that only 41 genes were

444 differentially expressed at both levels. Among them, only approximately 50% of genes
445 showed a consistent direction of fold change. When we compared DEGs and proteins
446 with different abundances (FC>2), 6 matches were obtained. A few studies have reported
447 a less than perfect correlation between transcript and protein expression, in Apicomplexan
448 [63,64] and mammalian systems [65,66]. The reasons for this phenomena are multiple
449 fold, including variations in protein degradation turn-over rates [67], differences in
450 posttranslational regulation [68], cellular functions [69] and last but not the least,
451 technical variations [70]. Despite the weak correlation found between the transcriptomic
452 and proteomic data in this work, transcriptome and proteome profiles highlight some
453 common distinctions among isolates.

454 Unfortunately, similarly to the proteomics results, a large portion (approximately 50%)
455 of these DEGs are annotated as hypothetical proteins or proteins with unknown function,
456 leading to a loss of interesting information. However, the transcriptome profiles showed
457 differences in tachyzoite-bradyzoite conversion, secretory elements, metabolism and
458 transcriptional regulation between isolates.

459 *Bradyzoite-specific genes were highly expressed in the Nc-Spain1H isolate.*

460 A remarkable result was the large number of bradyzoite-specific genes that were over-
461 expressed in the low virulent isolate Nc-Spain1H (Table 1). The gene encoding the
462 bradyzoite cytoplasmic antigen BAG1 (NCLIV_027470), which facilitates the transition
463 from the tachyzoite to bradyzoite in *T. gondii* [71] had the largest fold change between
464 isolates, demonstrating 140.6-fold higher expression in Nc-Spain1H. Other over-
465 expressed genes were the bradyzoite-specific surface antigens in *N. caninum* BSR4
466 (NCLIV_010030) and SAG4 (NCLIV_019580) [29,72]. Interestingly, as we have
467 previously commented, SAG4 protein was also more abundant in the Nc-Spain1H isolate
468 across the lytic cycle in this study. In addition to these stage-specific genes, the gene

469 related to early tachyzoite conversion into bradyzoites, PMA1 (NCLIV_022240) [73]
470 also displayed higher expression levels in the Nc-Spain1H isolate (23.6-fold). In addition,
471 some isoenzymes involved in glycolysis (lactate dehydrogenase, enolase, glucose 6-
472 phosphate isomerase) that are stage-specifically expressed in *T. gondii* and *N. caninum*
473 bradyzoites [59,74] such as LDH2 (NCLIV_042910) and ENO1 (NCLIV_037490) were
474 expressed at higher levels in Nc-Spain1H. The *N. caninum* gene orthologue of *T. gondii*
475 deoxyribose phosphate aldolase-like, which is involved in the utilization of deoxyribose
476 as a carbon and energy source in the bradyzoite stage [75], also exhibited higher
477 expression in the Nc-Spain1H isolate. Genes related to the tissue cyst wall, such as
478 NcMCP4 (NCLIV_003250) [76] and CST1 (NCLIV_040495), which play essential roles
479 in the structural integrity and persistence of brain cysts [77], had 12-fold and 40.3-fold
480 higher expression levels in the Nc-Spain1H isolate, respectively. Furthermore, higher
481 expression levels of ribosomal proteins have been associated with strains that readily
482 switch from the tachyzoite to bradyzoite in *T. gondii* [78]. This phenotype was also
483 observed in the low virulence Nc-Spain1H isolate since 23 ribosomal proteins showed
484 higher expression. It has been shown that Nc-Spain1H can start tachyzoite-bradyzoite
485 conversion *in vitro* under induction conditions, although it is not really completed to
486 encysted bradyzoites [32]. The bradyzoite-transcriptome and proteome profile expressed
487 by the Nc-Spain1H isolate could be related to its slower growth rate. Interestingly, *T.*
488 *gondii*, bradyzoite formation is preceded by, and critically dependent on, a parasite cell
489 cycle shift towards slower growth [31]. These early switching parasites have
490 transcriptomes that are very similar to those of tachyzoites, indicating that these early
491 developing parasites are largely slow-growing tachyzoites that can be considered pre-
492 bradyzoites [79]. This pre-bradyzoite stage in Nc-Spain1H may explain, at least partially,
493 its lower virulence in terms of causing abortion in cattle since tachyzoite growth (lower

494 in strains that tend to form bradyzoites) is a phenotypic trait related to virulence in *N.*
495 *caninum* and *T. gondii* [9,44,80].

496 *Host cell attachment and invasion machinery is also differentially expressed between*
497 *isolates.*

498 Seventeen genes encoding for SRS displayed higher abundances in the Nc-Spain1H
499 isolate, while only four were over-expressed in Nc-Spain7. These proteins are highly
500 immunogenic, and their expression is thought to regulate the virulence of infection [26].

501 In the proteome analyses, only five proteins demonstrated different abundances between
502 isolates, and the only one that matched between the transcriptome and proteome was the
503 bradyzoite antigen SAG4.

504 In contrast to the proteome results, the transcriptome analyses revealed fewer microneme
505 genes than SRS genes with differential expression between isolates. Seven had higher
506 expression in Nc-Spain1H and only 2 in Nc-Spain7. According to the proteome results,
507 MIC17B (NCLIV_038110) had higher expression in the Nc-Spain1H isolate. However,
508 the gene encoding the TLN4 protein, with an increased abundance in the Nc-Spain7
509 proteome at 56 hpi, was expressed at a higher level in the Nc-Spain1H isolate.

510 *Secretory effectors, rhoptry and dense granule proteins, also demonstrated differential*
511 *mRNA expression between isolates.*

512 Similarly to the proteomic results, the non-syntenic orthologue of *T. gondii* ROP24 was
513 more highly expressed in the highly virulent isolate Nc-Spain7, and the non-syntenic
514 orthologue of *T. gondii* ROP1 (NCLIV_069110) was more highly expressed in the low
515 virulent isolate Nc-Spain1H, but at 56 hpi instead of 12 hpi in the proteome. Another
516 rhoptry protein with elevated expression in Nc-Spain1H was the predicted lineage-
517 specific rhoptry kinase, subfamily ROPK-Eten1 (NCLIV_017420), which is present in
518 the *T. gondii* ROP38/29/19 gene locus that has been found to be necessary to establish

519 chronic infection in mice [81]. The only dense granule protein with differential expression
520 (2-fold higher in Nc-Spain7) was GRA17 (NCLIV_005560), which in *T. gondii* leads to
521 more rapid growth [82]. In the proteome studies, fewer differences were also found in
522 these proteins, and no GRA proteins were differentially expressed at 56 hpi.

523 In *T. gondii*, two different sub-transcriptomes have been described, depending on the
524 tachyzoite cell cycle phase. The G1-subtranscriptome characterized by the expression of
525 genes related to biosynthetic and metabolic functions and the S/M-subtranscriptome
526 enriched in specific genes for specialized apicomplexan processes, in which are included
527 SAG, MIC and ROP proteins [83]. Because the observed differences in proteome
528 elements and DNA transcription could be a consequence of a different progression across
529 the tachyzoite cell cycle, we examined the DNA content in asynchronously growing Nc-
530 Spain1H and Nc-Spain7 at 12, 36 and 56 hpi. At all time-points analysed, the flow
531 cytometry results for the tachyzoites profiles showed that most parasites were in G1 and
532 there were no differences between isolates (Fig. 5B), supporting a similar tachyzoite cell
533 cycle status at the studied time-points.

534 Although these results showing elevated expression of host cell attachment and invasion
535 machinery and secretory effectors related to virulence in the isolate with a reduced
536 invasion rate and virulence are quite surprising, a recent study has shown that the genes
537 encoding these functions also exhibited elevated expressions in the Nc-Spain1H isolate
538 at 12 hpi [16].

539 *Different ApiAP2 repertoire may lead to differences in RNA expression and proteomes.*

540 Although the mechanisms underlying gene-specific regulation in Apicomplexan parasites
541 are not completely known, the AP2 transcription factors in *T. gondii* have been associated
542 with important functions including stage-specific gene activation, determination of
543 differences between strains, parasite virulence and host invasion [78,79,84,85]. Most of

544 the identified ApiAP2s in *N. caninum* (54 out of 68) are expressed during the tachyzoite
545 stage, similar to *T. gondii* [27]. In our study, seven AP2 factors displayed higher
546 expression in the highly virulence isolate Nc-Spain7 (AP2VIII-3, AP2VIII-4, AP2IX-8,
547 AP2X-2, AP2X-11, AP2XI-1 and AP2XII-8) and two in the low virulence isolate Nc-
548 Spain1H (AP2III-1 and AP2X-10). In the proteome, by contrast, no AP2 factors exhibited
549 a differential abundance between isolates, which was likely due to lower sensitivity of the
550 technique in comparison to RNA-Seq. Some of these factors have been found to be
551 functional in stage-specific or cell cycle-regulated or even strain-specific expression in *T.*
552 *gondii* [79], and thus a similar characterization in *N. caninum* would be very useful to
553 better understand the regulation of gene expression in this parasite.

554 **4. Concluding remarks**

555 In this study, we performed proteome and transcriptome comparisons between two well-
556 characterized *N. caninum* isolates and established marked differences and revealed the
557 mechanisms potentially associated with phenotypic traits and virulence displayed by
558 these isolates. The invasion machinery, metabolism, response to stress and the tendency
559 to form bradyzoites have emerged as principal key factors for isolate behaviour and likely
560 pathogenesis. However, it should be noted that the majority of DEGs and proteins
561 between isolates were annotated as hypothetical and proteins with unknown function.
562 Enhancing the knowledge of this issue could be the best approach to unravel the
563 mechanisms underlying the molecular basis of the virulence of *N. caninum*.

564 Furthermore, the weak correlation between gene expression and protein abundance
565 highlighted the importance of post-transcriptional regulation in these parasites. High-
566 throughput proteomics techniques such as LC-MS/MS therefore offer a more detailed
567 picture than the transcriptome of mechanisms involved in phenotypic diversity and
568 virulence in *N. caninum*. However, proteome analyses are also limited by additional post-

569 transduction mechanisms involved in protein regulation (activation and protein turn
570 over). Nevertheless, despite the weak correlation between the transcript and protein at the
571 individual gene level, both datasets have identified, on a gene family level, a pre-
572 bradyzoite status of the Nc-Spain1H isolate. This observation is very interesting since it
573 could, at least partially, explain the reduced virulence of this isolate.

574 Altogether, the current study provides a global vision of the transcriptional and
575 translational differences between isolates that display marked virulence differences,
576 shedding light on a subset of proteins that are potentially involved in the pathogenesis of
577 this parasite. New studies with a battery of well-characterized isolates may reveal
578 common mechanism of *N. caninum* virulence. Our results lay the foundations for further
579 investigations characterizing the relevance of such proteins in *N. caninum* pathogenesis
580 and virulence.

581 **Conflict of interest statement**

582 The authors have declared no conflict of interest.

583 **Acknowledgements**

584 This work was supported by the Spanish Ministry of Economy and Competitiveness
585 (AGL2013-44694-R), the Community of Madrid (PLATESA S2013/ABI2906) and the
586 BBSRC (BB/L002477/1). The funders had no role in study design, data collection and
587 analysis, decision to publish, or preparation of the manuscript. We acknowledge Dr.
588 David Sibley from the Washington University School of Medicine (St. Louis, MO, USA)
589 for the NcMIC2 antibody, Dr. Andrew Hemphill from the Institute of Parasitology,
590 Vetsuisse Faculty (University of Bern, Switzerland) for the NcSAG1 antibody and Dra.
591 Aida Pitarch for advice in this work.

592 **Author contributions**

593 LMOM, JW, JRC, PH and ECF conceived and designed the experiments. JRC and PH
594 carried out the tachyzoite samples collection for analyses. DX and NR performed RNA-
595 Seq and LC/MS-MS analyses. PH performed the validation assays. DX performed
596 bioinformatics analyses. PH, JRC and DX analysed data and wrote the manuscript.
597 LMOM and NR critically revised the manuscript.

598

599 **References**

600 [1] J. Dubey, G. Schares, Neosporosis in animals—the last five years, *Vet. Parasitol.* 180
601 (2011) 90-108.

602 [2] M. P. Reichel, M. Alejandra Ayanegui-Alcérreca, L. F. P. Gondim, J. T. Ellis, What
603 is the global economic impact of *Neospora caninum* in cattle – The billion dollar question,
604 *Int. J. Parasitol.* 43 (2013) 133-42.

605 [3] A. L. Chryssafidis, G. Canton, F. Chianini, E. A. Innes, E. H. Madureira, S. M.
606 Gennari, Pathogenicity of Nc-Bahia and Nc-1 strains of *Neospora caninum* in
607 experimentally infected cows and buffaloes in early pregnancy, *Parasitol. Res.* 113 (2014)
608 1521-8.

609 [4] S. Rojo-Montejo, E. Collantes-Fernández, J. Blanco-Murcia, A. Rodríguez-Bertos, V.
610 Risco-Castillo, L. M. Ortega-Mora, Experimental infection with a low virulence isolate
611 of *Neospora caninum* at 70 days gestation in cattle did not result in foetopathy, *Vet. Res.*
612 40 (2009) 49.

613 [5] S. G. Caspe, D. P. Moore, M. R. Leunda, D. B. Cano, L. Lischinsky, J. Regidor-
614 Cerrillo, G. Álvarez-García, I. G. Echaide, D. Bacigalupe, L. M. Ortega-Mora, A. C.
615 Odeon, C. M. Campero, The *Neospora caninum*-Spain 7 isolate induces placental
616 damage, fetal death and abortion in cattle when inoculated in early gestation, *Vet.*
617 *Parasitol.* 189 (2012) 171-81.

618 [6] J. Regidor-Cerrillo, D. Arranz-Solís, J. Benavides, M. Gómez-Bautista, J. A. Castro-
619 Hermida, M. Mezo, V. Pérez, L. M. Ortega-Mora, M. González-Warleta, *Neospora*
620 *caninum* infection during early pregnancy in cattle: how the isolate influences infection
621 dynamics, clinical outcome and peripheral and local immune responses, *Vet. Res.* 45
622 (2014) 10,9716-45-10.

623 [7] A. Hemphill, B. Gottstein, H. Kaufmann, Adhesion and invasion of bovine endothelial
624 cells by *Neospora caninum*, *Parasitology* 112 (Pt 2) (1996) 183-97.

625 [8] A. Hemphill, N. Vonlaufen, A. Naguleswaran, N. Keller, M. Riesen, N. Guetg, S.
626 Srinivasan, F. Alaeddine, Tissue culture and explant approaches to studying and

- 627 visualizing *Neospora caninum* and its interactions with the host cell, *Microscopy and*
628 *Microanalysis* 10 (2004) 602-20.
- 629 [9] J. Regidor-Cerrillo, M. Gómez-Bautista, I. Sodupe, G. Aduriz, G. Álvarez-García, I.
630 Del Pozo, L. M. Ortega-Mora, In vitro invasion efficiency and intracellular proliferation
631 rate comprise virulence-related phenotypic traits of *Neospora caninum*, *Vet. Res.* 42
632 (2011) 41.
- 633 [10] A. Dellarupe, J. Regidor-Cerrillo, E. Jiménez-Ruiz, G. Schares, J. M. Unzaga, M. C.
634 Venturini, L. M. Ortega-Mora, Comparison of host cell invasion and proliferation among
635 *Neospora caninum* isolates obtained from oocysts and from clinical cases of naturally
636 infected dogs, *Exp. Parasitol.* 145 (2014) 22-8.
- 637 [11] L. Jiménez-Pelayo, M. García-Sánchez, J. Regidor-Cerrillo, P. Horcajo, E.
638 Collantes-Fernández, M. Gómez-Bautista, N. Hambruch, C. Pfarrer, L. M. Ortega-Mora,
639 Differential susceptibility of bovine caruncular and trophoblast cell lines to infection with
640 high and low virulence isolates of *Neospora caninum*, *Parasit. Vectors* 10 (2017) 463.
- 641 [12] H. Beck, D. Blake, M. Dardé, I. Felger, S. Pedraza-Díaz, J. Regidor-Cerrillo, M.
642 Gómez-Bautista, L. M. Ortega-Mora, L. Putignani, B. Shiels, A. Tait, W. Weir, Molecular
643 approaches to diversity of populations of apicomplexan parasites, *Int. J. Parasitol.* 39
644 (2009) 175-89.
- 645 [13] E. G. Lee, J. H. Kim, Y. S. Shin, G. W. Shin, Y. R. Kim, K. J. Palaksha, D. Y. Kim,
646 I. Yamane, Y. H. Kim, G. S. Kim, M. D. Suh, T. S. Jung, Application of proteomics for
647 comparison of proteome of *Neospora caninum* and *Toxoplasma gondii* tachyzoites, *J.*
648 *Chromatogr. B. Analyt. Technol. Biomed. Life Sci.* 815 (2005) 305-14.
- 649 [14] Y. S. Shin, G. W. Shin, Y. R. Kim, E. Y. Lee, H. H. Yang, K. J. Palaksha, H. J.
650 Youn, J. H. Kim, D. Y. Kim, A. E. Marsh, J. Lakritz, T. S. Jung, Comparison of proteome
651 and antigenic proteome between two *Neospora caninum* isolates, *Vet Parasitol* 134
652 (2005) 41-52.
- 653 [15] J. Regidor-Cerrillo, G. Álvarez-García, I. Pastor-Fernández, V. Marugán-Hernández,
654 M. Gómez-Bautista, L. M. Ortega-Mora, Proteome expression changes among virulent
655 and attenuated *Neospora caninum* isolates, *J. Proteomics* 75 (2012) 2306-18.
- 656 [16] P. Horcajo, L. Jiménez-Pelayo, M. García-Sánchez, J. Regidor-Cerrillo, E.
657 Collantes-Fernández, D. Rozas, N. Hambruch, C. Pfarrer, L. M. Ortega-Mora,
658 Transcriptome modulation of bovine trophoblast cells in vitro by *Neospora caninum*, *Int.*
659 *J. Parasitol.* 47 (2017) 791-9.
- 660 [17] J. Regidor-Cerrillo, M. Gómez-Bautista, J. Pereira-Bueno, G. Aduriz, V. Navarro-
661 Lozano, V. Risco-Castillo, A. Fernández-García, S. Pedraza-Díaz, L. M. Ortega-Mora,
662 Isolation and genetic characterization of *Neospora caninum* from asymptomatic calves in
663 Spain, *Parasitology* 135 (2008) 1651-9.
- 664 [18] J. A. Vizcaíno, A. Csordas, N. del-Toro, J. A. Dianes, J. Griss, I. Lavidas, G. Mayer,
665 Y. Perez-Riverol, F. Reisinger, T. Ternent, Q. W. Xu, R. Wang, H. Hermjakob, 2016
666 update of the PRIDE database and its related tools, *Nucleic Acids Res.* 44 (2016) 447-56.

- 667 [19] B. Gajria, A. Bahl, J. Brestelli, J. Dommer, S. Fischer, X. Gao, M. Heiges, J. Iodice,
668 J. C. Kissinger, A. J. Mackey, D. F. Pinney, D. S. Roos, C. J. Stoeckert Jr, H. Wang, B.
669 P. Brunk, ToxoDB: an integrated *Toxoplasma gondii* database resource, *Nucleic Acids*
670 *Res.* 36 (2008) 553-56.
- 671 [20] D. Xia, S. J. Sanderson, A. R. Jones, J. H. Prieto, J. R. Yates, E. Bromley, F. M.
672 Tomley, K. Lal, R. E. Sinden, B. P. Brunk, D. S. Roos, J. M. Wastling, The proteome of
673 *Toxoplasma gondii*: integration with the genome provides novel insights into gene
674 expression and annotation, *Genome Biol.* 9 (2008) R116.
- 675 [21] L. Sheiner, J. L. Demerly, N. Poulsen, W. L. Beatty, O. Lucas, M. S. Behnke, M. W.
676 White, B. Striepen, A systematic screen to discover and analyze apicoplast proteins
677 identifies a conserved and essential protein import factor, *PLoS Pathog.* 7 (2011)
678 e1002392.
- 679 [22] L. Pollo-Oliveira, H. Post, M. L. Acencio, N. Lemke, H. van den Toorn, V. Tragante,
680 A. J. Heck, A. F. Altelaar, A. P. Yatsuda, Unravelling the *Neospora caninum* secretome
681 through the secreted fraction (ESA) and quantification of the discharged tachyzoite using
682 high-resolution mass spectrometry-based proteomics, *Parasit. Vectors* 6 (2013) 335.
- 683 [23] I. Pastor-Fernández, J. Regidor-Cerrillo, G. Álvarez-García, V. Marugán-Hernández,
684 P. García-Lunar, A. Hemphill, L. M. Ortega-Mora, The tandemly repeated NTPase
685 (NTPDase) from *Neospora caninum* is a canonical dense granule protein whose RNA
686 expression, protein secretion and phosphorylation coincides with the tachyzoite egress,
687 *Parasit. Vectors* 9 (2016) 352.
- 688 [24] I. Pastor-Fernández, J. Regidor-Cerrillo, E. Jiménez-Ruiz, G. Álvarez-García, V.
689 Marugán-Hernández, A. Hemphill, L. M. Ortega-Mora, Characterization of the *Neospora*
690 *caninum* NcROP40 and NcROP2Fam-1 rhoptry proteins during the tachyzoite lytic cycle,
691 *Parasitology* 143 (2016) 97-113.
- 692 [25] UniProt Consortium, Activities at the Universal Protein Resource (UniProt), *Nucleic*
693 *Acids Res.* 42 (2014) 191-98.
- 694 [26] C. Lekutis, D. J. Ferguson, M. E. Grigg, M. Camps, J. C. Boothroyd, Surface
695 antigens of *Toxoplasma gondii*: variations on a theme, *Int. J. Parasitol.* 31 (2001) 1285-
696 92.
- 697 [27] A. J. Reid, S. J. Vermont, J. A. Cotton, D. Harris, G. A. Hill-Cawthorne, S. Konen-
698 Waisman, S. M. Latham, T. Mourier, R. Norton, M. A. Quail, M. Sanders, D.
699 Shanmugam, A. Sohal, J. D. Wasmuth, B. Brunk, M. E. Grigg, J. C. Howard, J. Parkinson,
700 D. S. Roos, A. J. Trees, M. Berriman, A. Pain, J. M. Wastling, Comparative genomics of
701 the apicomplexan parasites *Toxoplasma gondii* and *Neospora caninum*: Coccidia
702 differing in host range and transmission strategy, *PLoS Pathog.* 8 (2012) e1002567.
- 703 [28] Y. Adomako-Ankomah, G. M. Wier, A. L. Borges, H. E. Wand, J. P. Boyle,
704 Differential locus expansion distinguishes Toxoplasmatinae species and closely related
705 strains of *Toxoplasma gondii*, *MBio* 5 (2014) e01003-13.

- 706 [29] A. Fernández-García, V. Risco-Castillo, A. Zaballos, G. Álvarez-García, L. M.
707 Ortega-Mora, Identification and molecular cloning of the *Neospora caninum* SAG4 gene
708 specifically expressed at bradyzoite stage, Mol. Biochem. Parasitol. 146 (2006) 89-97.
- 709 [30] J. D. Wasmuth, V. Pszeny, S. Haile, E. M. Jansen, A. T. Gast, A. Sher, J. P. Boyle,
710 M. J. Boulanger, J. Parkinson, M. E. Grigg, Integrated bioinformatic and targeted deletion
711 analyses of the SRS gene superfamily identify SRS29C as a negative regulator of
712 *Toxoplasma* virulence, MBio 3 (2012) e00321-12.
- 713 [31] M. E. Jerome, J. R. Radke, W. Bohne, D. S. Roos, M. W. White, *Toxoplasma gondii*
714 bradyzoites form spontaneously during sporozoite-initiated development, Infect. Immun.
715 66 (1998) 4838-44.
- 716 [32] S. Rojo-Montejo, E. Collantes-Fernández, J. Regidor-Cerrillo, G. Álvarez-García,
717 V. Marugán-Hernández, S. Pedraza-Díaz, J. Blanco-Murcia, A. Prenafeta, L. M. Ortega-
718 Mora, Isolation and characterization of a bovine isolate of *Neospora caninum* with low
719 virulence, Vet. Parasitol. 159 (2009) 7-16.
- 720 [33] F. M. Tomley, D. S. Soldati, Mix and match modules: structure and function of
721 microneme proteins in apicomplexan parasites, Trends Parasitol. 17 (2001) 81-8.
- 722 [34] A. Naguleswaran, A. Cannas, N. Keller, N. Vonlaufen, G. Schares, F. J. Conraths,
723 C. Bjorkman, A. Hemphill, *Neospora caninum* microneme protein NcMIC3: secretion,
724 subcellular localization, and functional involvement in host cell interaction, Infect.
725 Immun. 69 (2001) 6483-94.
- 726 [35] N. Keller, A. Naguleswaran, A. Cannas, N. Vonlaufen, M. Bienz, C. Bjorkman, W.
727 Bohne, A. Hemphill, Identification of a *Neospora caninum* microneme protein (NcMIC1)
728 which interacts with sulfated host cell surface glycosaminoglycans, Infect. Immun. 70
729 (2002) 3187-98.
- 730 [36] N. Keller, M. Riesen, A. Naguleswaran, N. Vonlaufen, R. Stettler, A. Leepin, J. M.
731 Wastling, A. Hemphill, Identification and characterization of a *Neospora caninum*
732 microneme-associated protein (NcMIC4) that exhibits unique lactose-binding properties,
733 Infect. Immun. 72 (2004) 4791-800.
- 734 [37] J. Wang, D. Tang, W. Li, J. Xu, Q. Liu, J. Liu, A new microneme protein of *Neospora*
735 *caninum*, NcMIC8 is involved in host cell invasion, Exp. Parasitol. 175 (2017) 21-7.
- 736 [38] H. Zhang, M. K. Compaore, E. G. Lee, M. Liao, G. Zhang, C. Sugimoto, K. Fujisaki,
737 Y. Nishikawa, X. Xuan, Apical membrane antigen 1 is a cross-reactive antigen between
738 *Neospora caninum* and *Toxoplasma gondii*, and the anti-NcAMA1 antibody inhibits host
739 cell invasion by both parasites, Mol. Biochem. Parasitol. 151 (2007) 205-12.
- 740 [39] V. Lagal, E. M. Binder, M. H. Huynh, B. F. Kafsack, P. K. Harris, R. Diez, D. Chen,
741 R. N. Cole, V. B. Carruthers, K. Kim, *Toxoplasma gondii* protease TgSUB1 is required
742 for cell surface processing of micronemal adhesive complexes and efficient adhesion of
743 tachyzoites, Cell Microbiol. 12 (2010) 1792-808.

- 744 [40] F. Parussini, I. Coppens, P. P. Shah, S. L. Diamond, V. B. Carruthers, Cathepsin L
745 occupies a vacuolar compartment and is a protein maturase within the endo/exocytic
746 system of *Toxoplasma gondii*, Mol. Microbiol. 76 (2010) 1340-57.
- 747 [41] M. S. Roiko, V. B. Carruthers, Functional dissection of *Toxoplasma gondii* perforin-
748 like protein 1 reveals a dual domain mode of membrane binding for cytolysis and parasite
749 egress, J. Biol. Chem. 288 (2013) 8712-25.
- 750 [42] F. Almeida, A. Sardinha-Silva, T. A. da Silva, A. M. Pessoni, C. F. Pinzan, A. C.
751 Alegre-Maller, N. T. Cecilio, N. S. Moretti, A. R. Damasio, W. R. Pedersoli, J. R. Mineo,
752 R. N. Silva, M. C. Roque-Barreira, *Toxoplasma gondii* Chitinase induces macrophage
753 activation, PLoS One 10 (2015) e0144507.
- 754 [43] M. A. Hakimi, P. Olias, L. D. Sibley, *Toxoplasma* effectors targeting host signaling
755 and transcription, Clin. Microbiol. Rev. 30 (2017) 615-45.
- 756 [44] L. D. Sibley, W. Qiu, S. Fentress, S. J. Taylor, A. Khan, R. Hui, Forward genetics in
757 *Toxoplasma gondii* reveals a family of rhoptry kinases that mediates pathogenesis,
758 Eukaryot. Cell 8 (2009) 1085-93.
- 759 [45] P. N. Ossorio, J. D. Schwartzman, J. C. Boothroyd, A *Toxoplasma gondii* rhoptry
760 protein associated with host cell penetration has unusual charge asymmetry, Mol.
761 Biochem. Parasitol. 50 (1992) 1-15.
- 762 [46] K. R. Buchholz, P. W. Bowyer, J. C. Boothroyd, Bradyzoite pseudokinase 1 is crucial
763 for efficient oral infectivity of the *Toxoplasma gondii* tissue cyst, Eukaryot. Cell 12
764 (2013) 399-410.
- 765 [47] M. Blume, R. Nitzsche, U. Sternberg, M. Gerlic, S. L. Masters, N. Gupta, M. J.
766 McConville, A *Toxoplasma gondii* gluconeogenic enzyme contributes to robust central
767 carbon metabolism and is essential for replication and virulence, Cell Host Microbe 18
768 (2015) 210-20.
- 769 [48] A. M. Guggisberg, A. R. Odom, Sweet talk: regulating glucose metabolism in
770 *Toxoplasma*, Cell Host Microbe 18 (2015) 142-3.
- 771 [49] G. I. McFadden, E. Yeh, The apicoplast: now you see it, now you don't, Int. J.
772 Parasitol. 47 (2017) 137-44.
- 773 [50] C. F. Brooks, H. Johnsen, G. G. van Dooren, M. Muthalagi, S. S. Lin, W. Bohne, K.
774 Fischer, B. Striepen, The *toxoplasma* apicoplast phosphate translocator links cytosolic
775 and apicoplast metabolism and is essential for parasite survival, Cell Host Microbe 7
776 (2010) 62-73.
- 777 [51] C. Song, M. A. Chiasson, N. Nursimulu, S. S. Hung, J. Wasmuth, M. E. Grigg, J.
778 Parkinson, Metabolic reconstruction identifies strain-specific regulation of virulence in
779 *Toxoplasma gondii*, Mol. Syst. Biol. 9 (2013) 708.

- 780 [52] T. Tanaka, H. Nagasawa, K. Fujisaki, N. Suzuki, T. Mikami, Growth-inhibitory
781 effects of interferon-gamma on *Neospora caninum* in murine macrophages by a nitric
782 oxide mechanism, *Parasitol. Res.* 86 (2000) 768-71.
- 783 [53] S. S. Bosch, T. Kronenberger, K. A. Meissner, F. M. Zimbres, D. Stegehake, N. M.
784 Izui, I. Schettert, E. Liebau, C. Wrenger, Oxidative stress control by apicomplexan
785 parasites, *Biomed. Res. Int.* 2015 (2015) 351289.
- 786 [54] P. Pino, B. J. Foth, L. Y. Kwok, L. Sheiner, R. Schepers, T. Soldati, D. Soldati-Favre,
787 Dual targeting of antioxidant and metabolic enzymes to the mitochondrion and the
788 apicoplast of *Toxoplasma gondii*, *PLoS Pathog.* 3 (2007) e115.
- 789 [55] M. W. Robinson, A. T. Hutchinson, J. P. Dalton, S. Donnelly, Peroxiredoxin: a
790 central player in immune modulation, *Parasite Immunol.* 32 (2010) 305-13.
- 791 [56] R. M. Fereig, Y. Nishikawa, Peroxiredoxin 3 promotes IL-12 production from
792 macrophages and partially protects mice against infection with *Toxoplasma gondii*,
793 *Parasitol. Int.* 65 (2016) 741-8.
- 794 [57] L. M. Weiss, Y. F. Ma, P. M. Takvorian, H. B. Tanowitz, M. Wittner, Bradyzoite
795 development in *Toxoplasma gondii* and the hsp70 stress response, *Infect. Immun.* 66
796 (1998) 3295-302.
- 797 [58] P. C. Echeverria, M. Matrajt, O. S. Harb, M. P. Zappia, M. A. Costas, D. S. Roos, J.
798 F. Dubremetz, S. O. Angel, *Toxoplasma gondii* Hsp90 is a potential drug target whose
799 expression and subcellular localization are developmentally regulated, *J. Mol. Biol.* 350
800 (2005) 723-34.
- 801 [59] V. Marugán-Hernández, G. Álvarez-García, V. Risco-Castillo, J. Regidor-Cerrillo,
802 L. M. Ortega-Mora, Identification of *Neospora caninum* proteins regulated during the
803 differentiation process from tachyzoite to bradyzoite stage by DIGE, *Proteomics* 10
804 (2010) 1740-50.
- 805 [60] N. de Miguel, P. C. Echeverria, S. O. Angel, Differential subcellular localization of
806 members of the *Toxoplasma gondii* small heat shock protein family, *Eukaryot Cell* 4
807 (2005) 1990-7.
- 808 [61] C. Muñoz, J. San Francisco, B. Gutiérrez, J. González, Role of the ubiquitin-
809 proteasome systems in the biology and virulence of protozoan parasites, *Biomed. Res.*
810 *Int.* 2015 (2015) 141526.
- 811 [62] N. C. Silmon de Monerri, R. R. Yakubu, A. L. Chen, P. J. Bradley, E. Nieves, L. M.
812 Weiss, K. Kim, The Ubiquitin proteome of *Toxoplasma gondii* reveals roles for protein
813 ubiquitination in cell-cycle transitions, *Cell Host Microbe* 18 (2015) 621-33.
- 814 [63] T. W. Kooij, C. J. Janse, A. P. Waters, *Plasmodium* post-genomics: better the bug
815 you know? *Nat. Rev. Microbiol.* 4 (2006) 344-57.

- 816 [64] J. M. Wastling, D. Xia, A. Sohal, M. Chaussepied, A. Pain, G. Langsley, Proteomes
817 and transcriptomes of the Apicomplexa--where's the message? *Int. J. Parasitol.* 39 (2009)
818 135-43.
- 819 [65] T. Maier, M. Guell, L. Serrano, Correlation of mRNA and protein in complex
820 biological samples, *FEBS Lett.* 583 (2009) 3966-73.
- 821 [66] R. de Sousa Abreu, L. O. Penalva, E. M. Marcotte, C. Vogel, Global signatures of
822 protein and mRNA expression levels, *Mol. Biosyst.* 5 (2009) 1512-26.
- 823 [67] B. Schwanhausser, D. Busse, N. Li, G. Dittmar, J. Schuchhardt, J. Wolf, W. Chen,
824 M. Selbach, Global quantification of mammalian gene expression control, *Nature* 473
825 (2011) 337-42.
- 826 [68] A. Battle, Z. Khan, S. H. Wang, A. Mitrano, M. J. Ford, J. K. Pritchard, Y. Gilad,
827 Genomic variation. Impact of regulatory variation from RNA to protein, *Science* 347
828 (2015) 664-7.
- 829 [69] M. Jovanovic, M. S. Rooney, P. Mertins, D. Przybylski, N. Chevrier, R. Satija, E. H.
830 Rodriguez, A. P. Fields, S. Schwartz, R. Raychowdhury, M. R. Mumbach, T. Eisenhaure,
831 M. Rabani, D. Gennert, D. Lu, T. Delorey, J. S. Weissman, S. A. Carr, N. Hacohen, A.
832 Regev, Immunogenetics. Dynamic profiling of the protein life cycle in response to
833 pathogens, *Science* 347 (2015) 1259038.
- 834 [70] J. J. Li, P. J. Bickel, M. D. Biggin, System wide analyses have underestimated protein
835 abundances and the importance of transcription in mammals, *PeerJ* 2 (2014) e270.
- 836 [71] Y. W. Zhang, K. Kim, Y. F. Ma, M. Wittner, H. B. Tanowitz, L. M. Weiss,
837 Disruption of the *Toxoplasma gondii* bradyzoite-specific gene BAG1 decreases in vivo
838 cyst formation, *Mol. Microbiol.* 31 (1999) 691-701.
- 839 [72] V. Risco-Castillo, A. Fernández-García, A. Zaballos, A. Aguado-Martínez, A.
840 Hemphill, A. Rodríguez-Bertos, G. Álvarez-García, L. M. Ortega-Mora, Molecular
841 characterisation of BSR4, a novel bradyzoite-specific gene from *Neospora caninum*, *Int.*
842 *J. Parasitol.* 37 (2007) 887-96.
- 843 [73] M. Holpert, U. Gross, W. Bohne, Disruption of the bradyzoite-specific P-type (H+)-
844 ATPase PMA1 in *Toxoplasma gondii* leads to decreased bradyzoite differentiation after
845 stress stimuli but does not interfere with mature tissue cyst formation, *Mol. Biochem.*
846 *Parasitol.* 146 (2006) 129-33.
- 847 [74] S. Tomavo, The differential expression of multiple isoenzyme forms during stage
848 conversion of *Toxoplasma gondii*: an adaptive developmental strategy, *Int. J. Parasitol.*
849 31 (2001) 1023-31.
- 850 [75] A. Ueno, G. Dautu, B. Munyaka, G. Carmen, Y. Kobayashi, M. Igarashi,
851 *Toxoplasma gondii*: Identification and characterization of bradyzoite-specific
852 deoxyribose phosphate aldolase-like gene (TgDPA), *Exp. Parasitol.* 121 (2009) 55-63.

- 853 [76] K. R. Buchholz, H. M. Fritz, X. Chen, B. Durbin-Johnson, D. M. Rocke, D. J.
854 Ferguson, P. A. Conrad, J. C. Boothroyd, Identification of tissue cyst wall components
855 by transcriptome analysis of in vivo and in vitro *Toxoplasma gondii* bradyzoites,
856 Eukaryot. Cell 10 (2011) 1637-47.
- 857 [77] T. Tomita, D. J. Bzik, Y. F. Ma, B. A. Fox, L. M. Markillie, R. C. Taylor, K. Kim,
858 L. M. Weiss, The *Toxoplasma gondii* cyst wall protein CST1 is critical for cyst wall
859 integrity and promotes bradyzoite persistence, PLoS Pathog. 9 (2013) e1003823.
- 860 [78] M. M. Croken, Y. Ma, L. M. Markillie, R. C. Taylor, G. Orr, L. M. Weiss, K. Kim,
861 Distinct strains of *Toxoplasma gondii* feature divergent transcriptomes regardless of
862 developmental stage, PLoS One 9 (2014) e111297.
- 863 [79] D. P. Hong, J. B. Radke, M. W. White, Opposing transcriptional mechanisms
864 regulate *Toxoplasma* development, mSphere 2 (2017) e00347-16.
- 865 [80] J. P. Saeij, J. P. Boyle, J. C. Boothroyd, Differences among the three major strains
866 of *Toxoplasma gondii* and their specific interactions with the infected host, Trends
867 Parasitol. 21 (2005) 476-81.
- 868 [81] B. A. Fox, L. M. Rommereim, R. B. Guevara, A. Falla, M. A. Hortua Triana, Y. Sun,
869 D. J. Bzik, The *Toxoplasma gondii* rhoptry kinome is essential for chronic infection,
870 MBio 7 (2016) e00193-16.
- 871 [82] D. A. Gold, A. D. Kaplan, A. Lis, G. C. Bett, E. E. Rosowski, K. M. Cirelli, A.
872 Bougdour, S. M. Sidik, J. R. Beck, S. Lourido, P. F. Egea, P. J. Bradley, M. A. Hakimi,
873 R. L. Rasmusson, J. P. Saeij, The *Toxoplasma* dense granule proteins GRA17 and GRA23
874 mediate the movement of small molecules between the host and the parasitophorous
875 vacuole, Cell Host Microbe 17 (2015) 642-52.
- 876 [83] M. S. Behnke, J. C. Wootton, M. M. Lehmann, J. B. Radke, O. Lucas, J. Nawas, L.
877 D. Sibley, M. W. White, Coordinated progression through two subtranscriptomes
878 underlies the tachyzoite cycle of *Toxoplasma gondii*, PLoS One 5 (2010) e12354.
- 879 [84] R. Walker, M. Gissot, M. M. Croken, L. Huot, D. Hot, K. Kim, S. Tomavo, The
880 *Toxoplasma* nuclear factor TgAP2XI-4 controls bradyzoite gene expression and cyst
881 formation, Mol. Microbiol. 87 (2013) 641-55.
- 882 [85] R. Walker, M. Gissot, L. Huot, T. D. Alayi, D. Hot, G. Marot, C. Schaeffer-Reiss,
883 A. Van Dorsselaer, K. Kim, S. Tomavo, *Toxoplasma* transcription factor TgAP2XI-5
884 regulates the expression of genes involved in parasite virulence and host invasion, J. Biol.
885 Chem. 288 (2013) 31127-38.

886

887 **Figure legends**

888 **Figure 1. Experimental design of the proteome and transcriptome analyses.** Samples
889 for proteome and transcriptome analyses were assayed in triplicate. (A)

890 Photomicrographs for each time-point of sample collection at 400x. Black arrows indicate
891 parasitophorous vacuoles at 12, 36 and 56 hpi. Red arrows indicate an area of recent
892 egress. (B) Experimental design for proteome analyses. Tachyzoites were collected at 12,
893 36 and 56 hpi and purified using PD-10 columns. Purified tachyzoites were digested and
894 analysed on an Easy-Spray column fused to a silica nanoelectrospray emitter coupled to
895 a Q-Exactive mass spectrometer. For proteome data analyses, Progenesis QI (version 2.0,
896 Nonlinear Dynamics) and Mascot (version 2.3, Matrix Science) for peptide identification
897 were used. (C) Experimental design for transcript analyses. Total RNA was isolated from
898 purified tachyzoites, and then polyadenylated RNA was purified and used to prepare
899 RNA-seq libraries. Libraries were sequenced with HiSeq2500. The TopHat2 aligner was
900 used to align sequencing reads against the reference genome, and the Cufflinks software
901 (version 2.1.1) was applied to assemble transcripts, quantify expression levels and analyse
902 differentially expressed genes.

903 **Figure 2: Volcano plot showing the proteome results.** (A) Volcano plot of
904 differentially abundant proteins at 12 hpi. (B) Volcano plot of differentially abundant
905 proteins at 36 hpi. (C) Volcano plot of differentially abundant proteins at 56 hpi. The 'x'
906 axis represents the \log_2 fold-change of different protein abundances (Nc-Spain1H vs Nc-
907 Spain7), and 'y' axis represents the negative \log_{10} of the p value. Proteins have been
908 grouped and coloured in the main categories: host attachment and invasion in red,
909 metabolic processes in green, other biological systems in purple and unannotated proteins
910 in grey. The dotted line represents the position of the fold change = 2, from which the
911 differences in abundance are considered significant.

912 **Figure 3. Venn diagrams showing the number of differentially abundant proteins**
913 **between Nc-Spain1H and Nc-Spain7 isolates across tachyzoite lytic cycle.** (A) The
914 total number of proteins increased in abundance (fold change ≥ 2) in the Nc-Spain1H

915 isolate each time-point of the lytic cycle (12 hpi, 36 hpi and 56 hpi). (B) The total number
916 of proteins increased in abundance (fold change ≥ 2) in the Nc-Spain7 isolate at 12 hpi,
917 36 hpi and 56 hpi. Proteins are listed in Supplemental file 4.

918 **Figure 4. Number of proteins with higher abundance in each isolate grouped in**
919 **functional categories.** (A) Number of proteins with higher abundance in each isolate at
920 12 hpi, (B) number of proteins with higher abundance in each isolate at 36 hpi and (C)
921 number of proteins with higher abundance in each isolate at 56 hpi.

922 **Figure 5: Invasion rates and flow cytometry profiles of Nc-Spain1H and Nc-Spain7**
923 **tachyzoites.** (A) Graphs represent parasite infection rates defined as the percentage of
924 invaded tachyzoites. Bars represent median invasion rates, and each point represents
925 invasion rates determined for 4 replicates from 3 independent assays. (**) indicates $P <$
926 0.01 (Mann-Whitney U-test). (B) Representative flow cytometric histograms showing the
927 distribution of tachyzoites in each cell cycle phase using a propidium iodide stain. The
928 table shows the average percentages of G1 and G2/M tachyzoites. The green lines show
929 the Nc-Spain7 isolate, and the black lines show the Nc-Spain1H isolate.

930 **Supplemental figure 1.** Predicted subcellular localization and functional classification
931 of identified proteins (A and B, respectively). Proteins were assigned a subcellular
932 localization or functional category combining the results of gene descriptions and Gene
933 Ontology annotation of *N. caninum* provided by ToxoDB. When no information was
934 available, the subcellular localization was predicted using GO annotation in syntenic
935 homologues from the *T. gondii* database and literature searches [20-22]. A detailed list of
936 proteins in each subcellular localization or functional category to accompany this figure
937 is provided in supplemental file 2. The numbers in the pie chart legends correspond to the
938 number of identified proteins in each category.

939 **Supplemental figure 2. Proteome validation by Western blot analyses.** Different
940 abundances of NcMIC2, NcROP2 and NcNTPase in Nc-Spain1H and Nc-Spain7 were
941 analysed by Western blot analyses. Total protein extracts from cultures infected with Nc-
942 Spain1H and Nc-Spain7 collected at 12, 36 and 56 hpi were electrophoresed in bis-
943 acrylamide gels and transferred onto PVDF membranes. For WB analyses rabbit
944 polyclonal anti-serum against NcMIC2, NcROP2, NcNTPase and NcSAG1 and goat anti-
945 rabbit IgG antibody conjugated to peroxidase, as a secondary antibody, were used. Note
946 that SAG1 was used in all cases as a housekeeping gene to normalize the amount of
947 tachyzoite protein in each sample. Expression levels of proteins were assessed by density
948 values (sum of pixel intensities by pixel area) using Quantity One quantification software
949 v. 4.0. The graphics show the protein expression differences that were determined from
950 the intensity ratios obtained for the different protein samples for each isolate.

951 **Supplemental figure 3. Validation of RNA-seq analyses by qPCR.** The graphic shows
952 the fold changes in the expression of *N. caninum* genes in the comparison of Nc-Spain7
953 vs Nc-Spain1H. Red columns show the results of the RNA-seq analyses, and green
954 columns the the qPCR results using SAG1 as the housekeeping gene. ¹Predicted member
955 of the rhoptry kinase family (ROPK), subfamily ROP20, ²orthologue of
956 TGME49_206510 toxolysin TLN4, ³putative retinitis pigmentosa GTPase regulator, and
957 ⁴hypothetical protein.

958 **Supplemental file 1.** Materials and methods. Detailed description of the materials and
959 methods sections: 1) LC-MS/MS analyses, 2) Western blot validation, 4) RNA-seq
960 analyses and 4) transcriptome validation by qPCR.

961 **Supplemental file 2.** Predicted subcellular localization and functional classification of
962 identified proteins from the tachyzoite proteome. Classification according to the gene
963 descriptions and Gene Ontology annotation of *N. caninum* provided by ToxoDB and,

964 when no information was available, from GO annotation in syntenic homologues from
965 the *T. gondii* database and literature searches [20-22].

966 **Supplemental file 3.** Proteins with different abundances between the Nc-Spain1H and
967 Nc-Spain7 proteomes.

968 **Supplemental file 4.** List of proteins belonging to each region of the Venn diagram
969 represented in Figure 3, showing the number of differentially abundant proteins between
970 Nc-Spain1H and Nc-Spain7 isolates across the tachyzoite lytic cycle.

971 **Supplemental file 5.** Transcriptome results.

972 Table 1. Bradyzoite-related genes with higher expression in Nc-Spain1H isolate.

Gene ID ¹	Ortholog in <i>T. gondii</i>	Gene Product	Fold change ²
NCLIV_027470	TGME49_259020	BAG1*	142.65
NCLIV_010030	TGME49_320230	BSR4	3.9
NCLIV_019580	TGME49_280570	SAG4	36.39
NCLIV_022240	TGME49_252640	PMA1*	23.6
NCLIV_042910	TGME49_291040	LDH2*	114.14
NCLIV_037490	TGME49_268860	ENO1*	23.22
NCLIV_010810	TGME49_318750	Deoxyribose-phosphate aldolase	42.61
NCLIV_003250	TGME49_208730	NcMCP4	11.97
NCLIV_040495	TGME49_264670	CST1*	40.29

973 ¹In addition to these genes, 23 ribosomal proteins had increased its expression in Nc-Sapin1H, a higher expression level
 974 of ribosomal proteins have been associated with strains that readily switch from tachyzoite to bradyzoite in *T. gondii*
 975 [78].

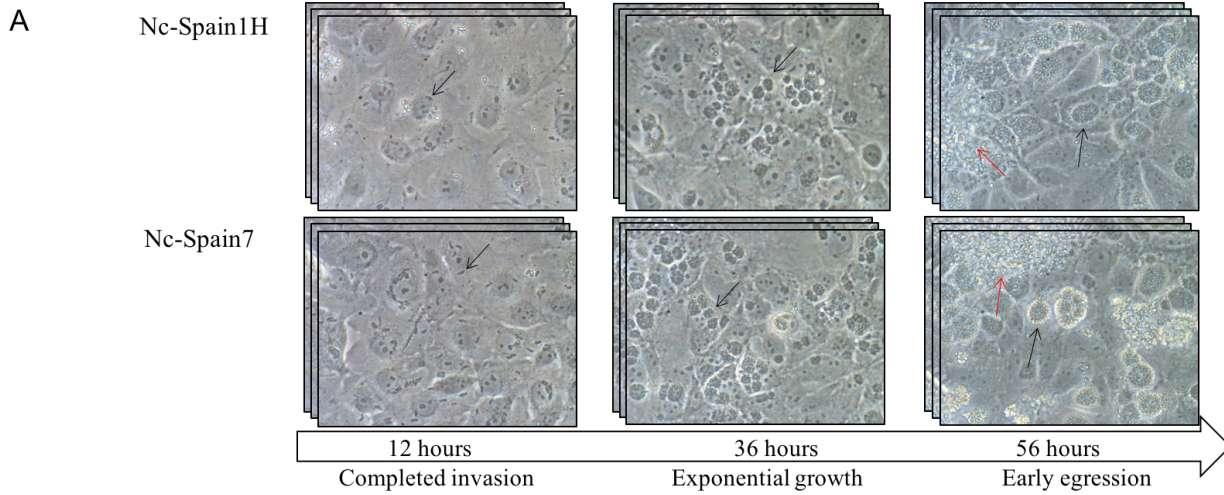
976 *Protein names are assigned from *T. gondii* orthologues because lack of *N. caninum* annotations

977 ²Fold change of the expression levels in the Nc-Spain1H comparing to Nc-Spain7

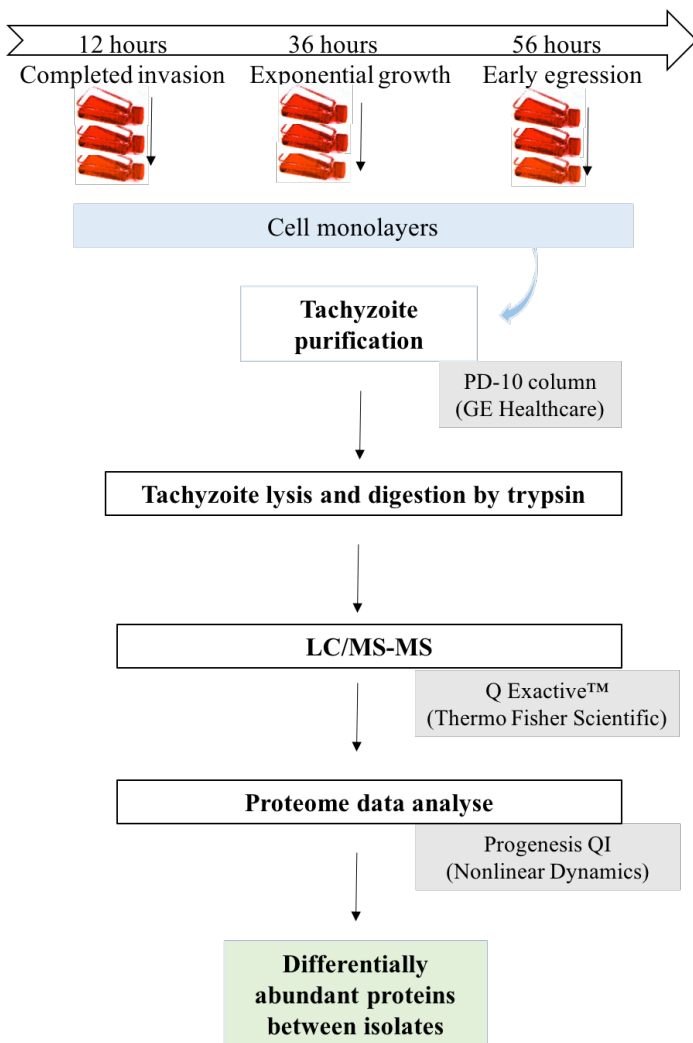
978

979

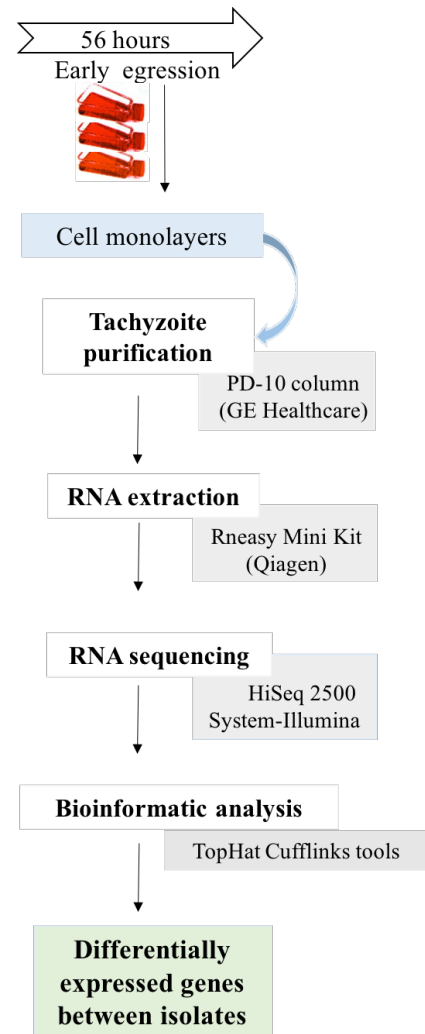
980



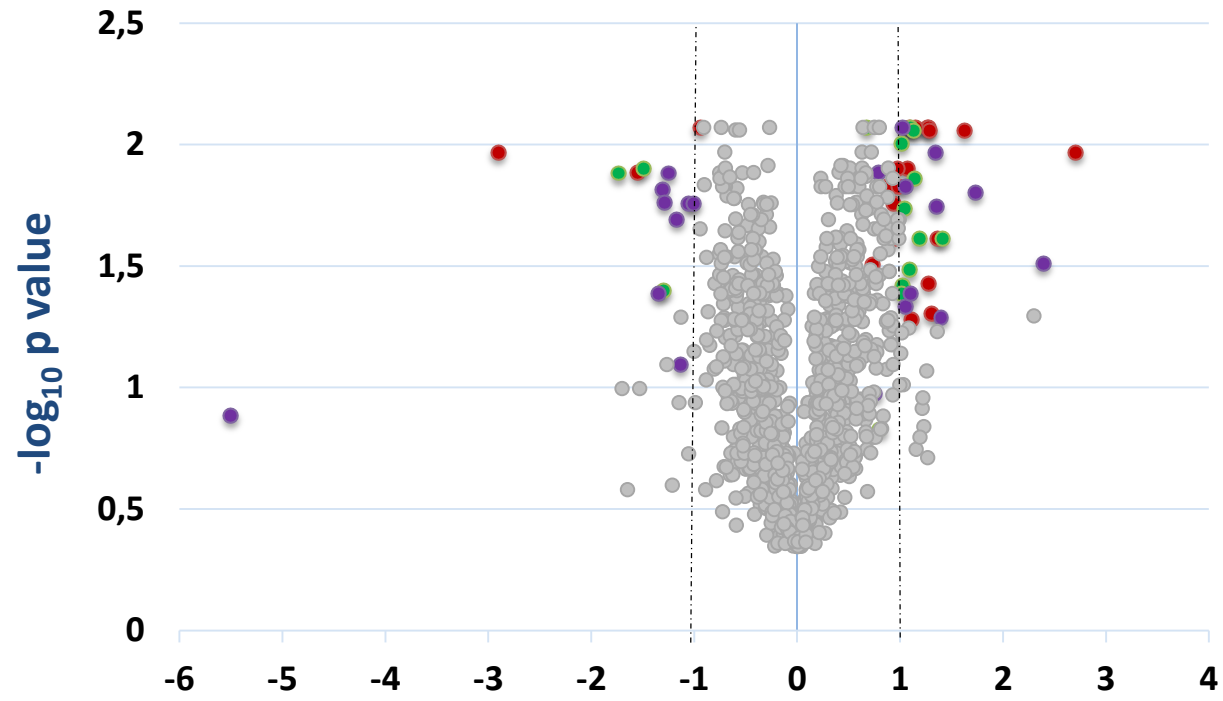
B



C

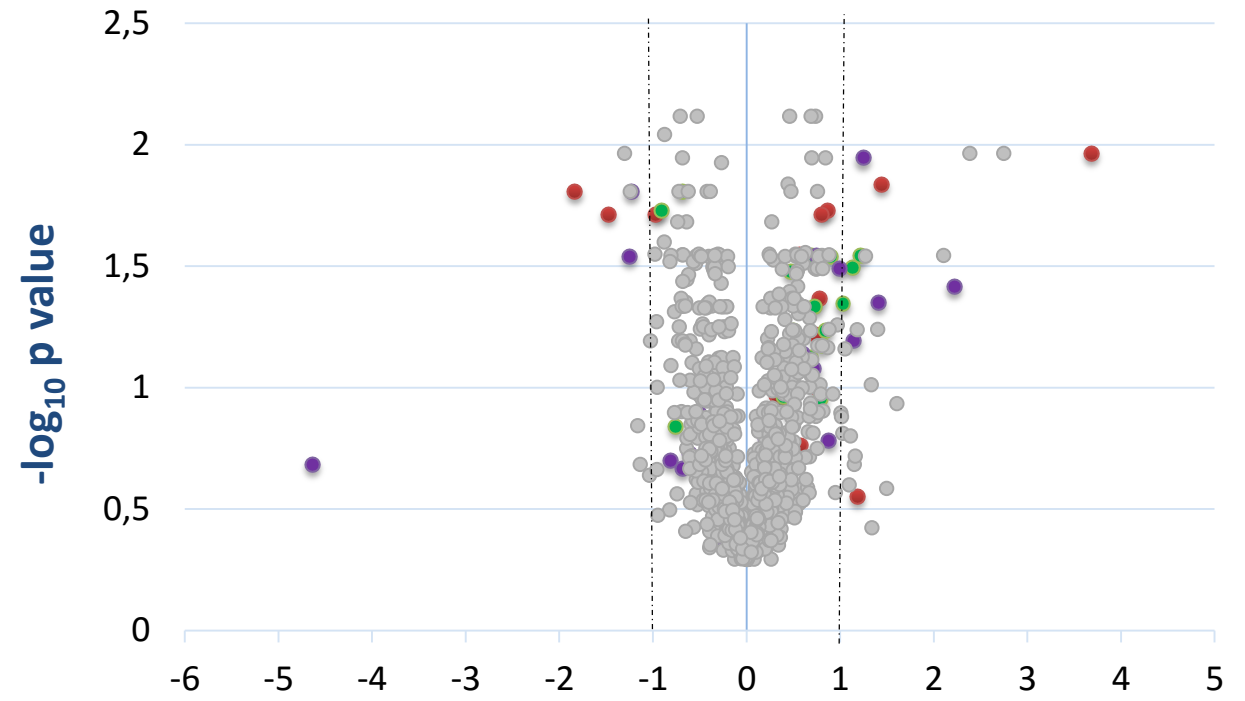


Proteome 12 hpi



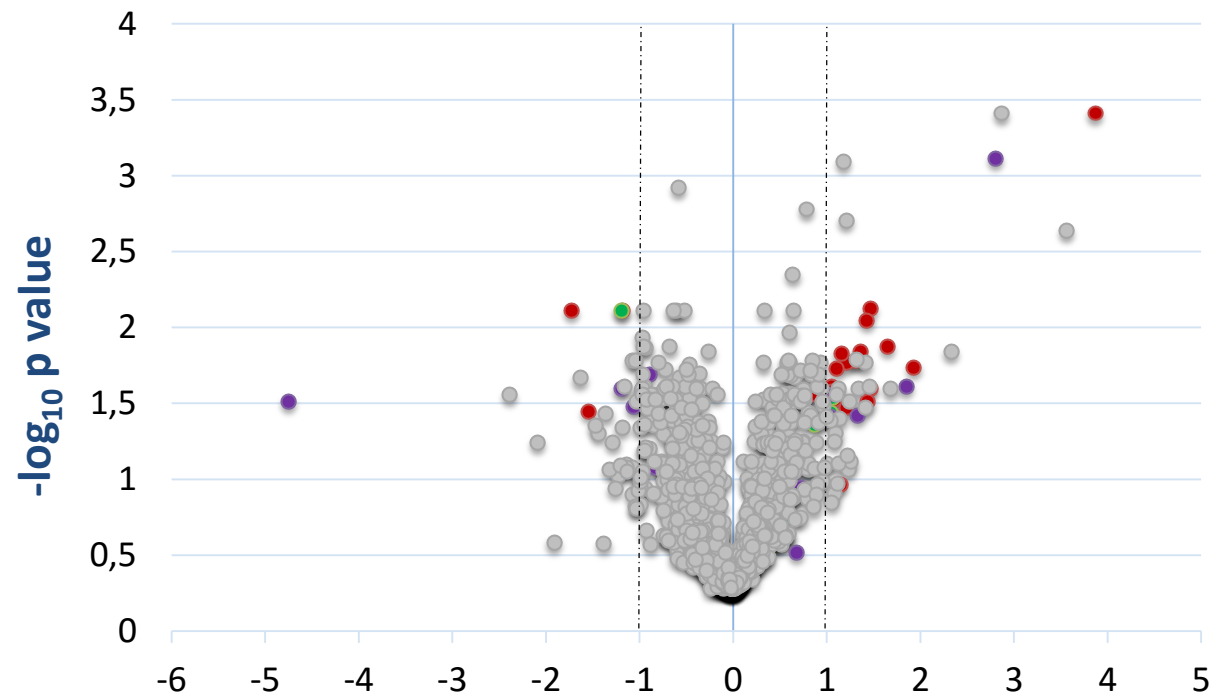
Nc-Spain1H vs Nc-Spain7 ($\log_2 \text{ FC}$)

Proteome 36 hpi



Nc-Spain1H vs Nc-Spain7 ($\log_2 \text{ FC}$)

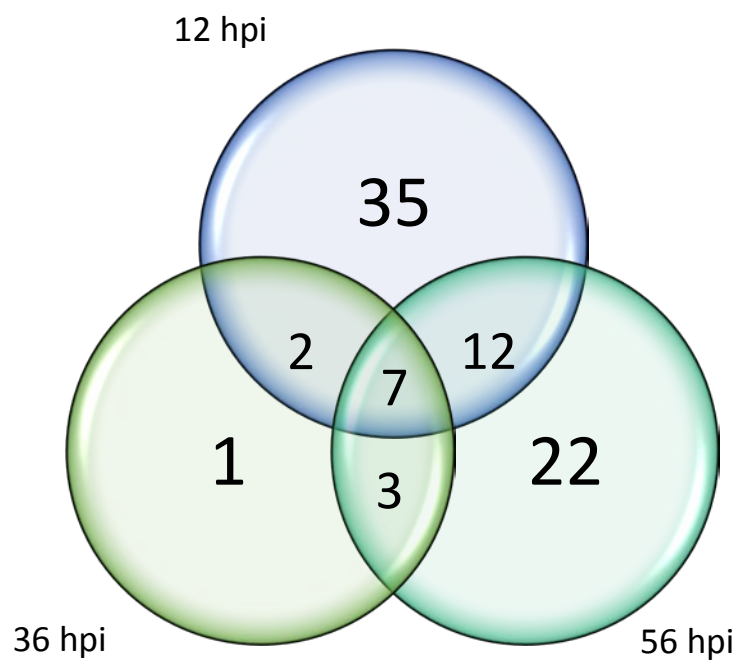
Proteome 56 hpi



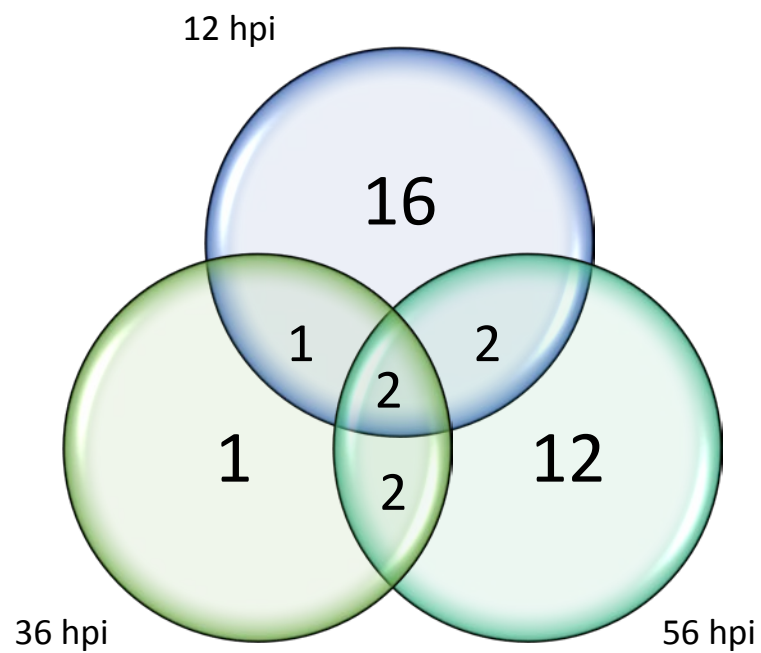
Nc-Spain1H vs Nc-Spain7 ($\log_2 \text{ FC}$)

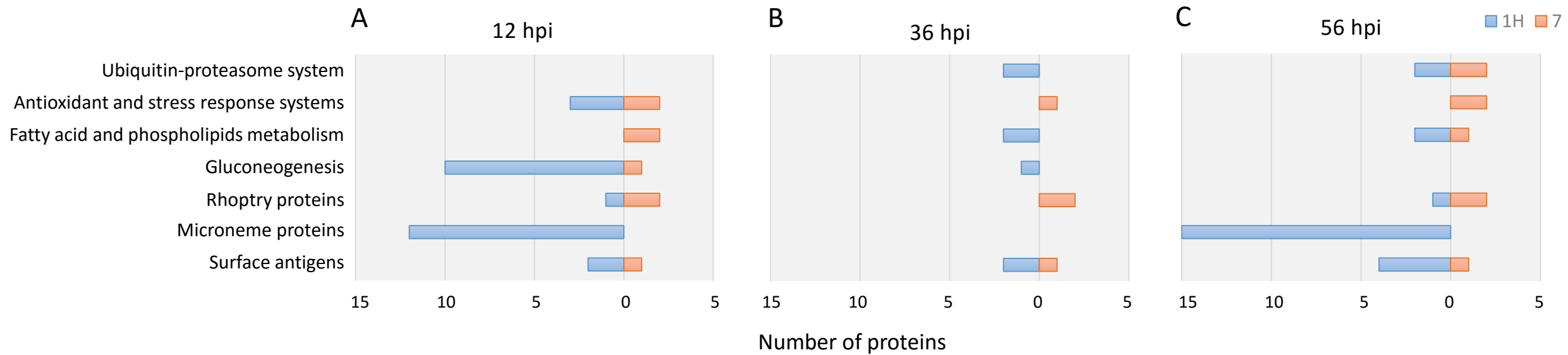
- Host attachment and invasion
- Metabolic processes
- Other biological systems
- Unannotated

A

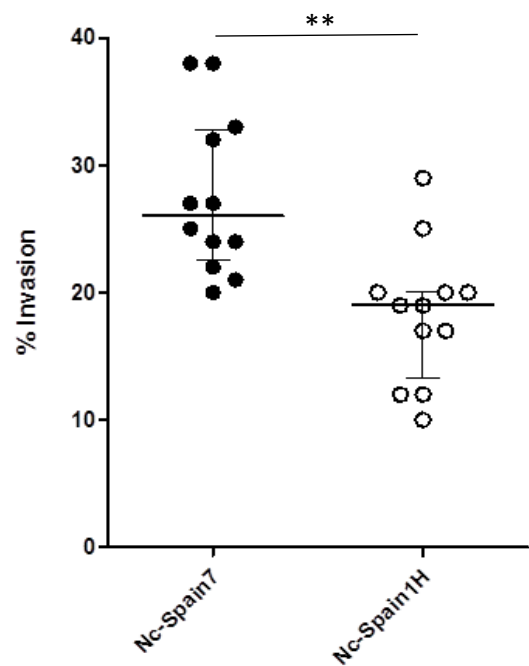


B

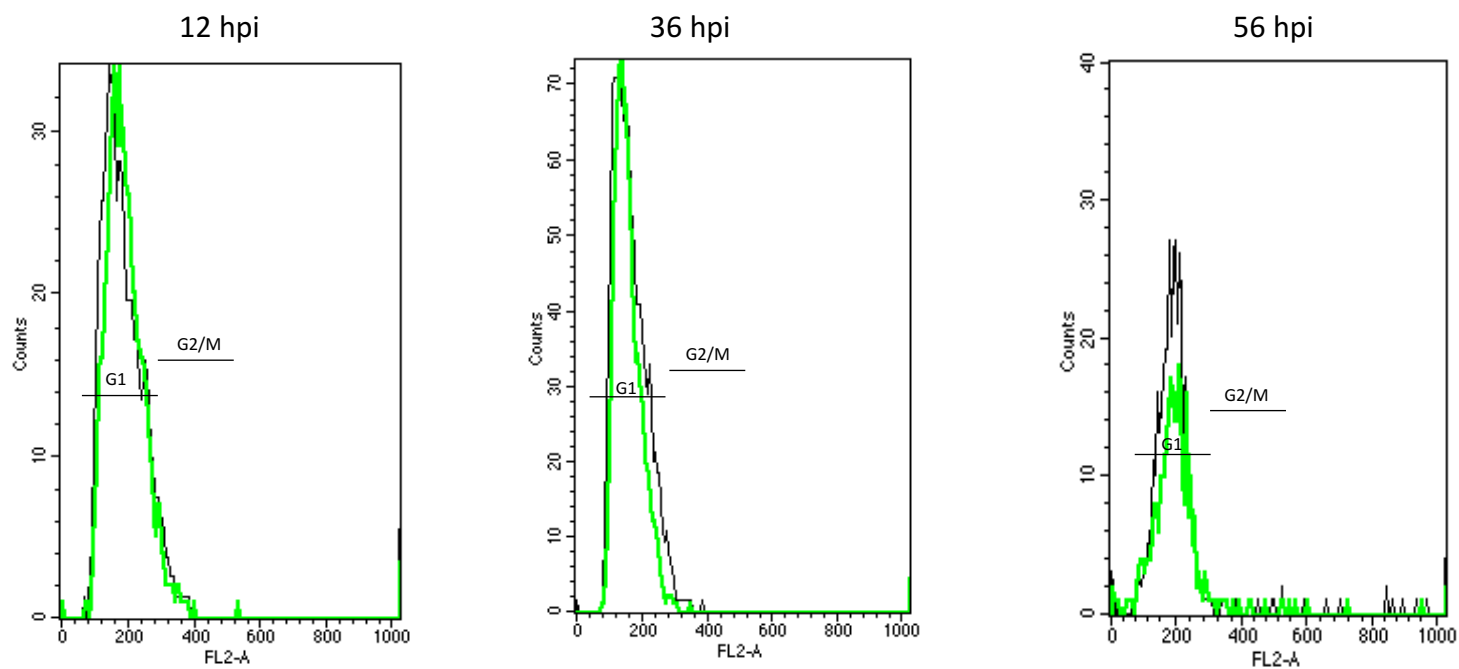




A



B



	G1	G2/M
NcSpain1H	97,22	2,01
NcSpain7	95,7	3,4

	G1	G2/M
NcSpain1H	98,41	1,14
NcSpain7	98,84	0,53

	G1	G2/M
NcSpain1H	85,9	14,1
NcSpain7	88,4	11,1